



FDR4ALT



Validation Report Document Atmosphere TDP



CLS-ENV-NT-23-0425

Issue 4.1 – 04/07/2023

Public

AUTHORS TABLE

Object	Name
Authors	Frank Fell, Ralf Bennartz (Informus), Bruno Picard (FLUCTUS), Mathilde Siméon, Marie-Laure Fréry, Fanny Piras (CLS)
Checked by	Gabriele Brizzi (SERCO) and Pierre Féménias (ESA)
Accepted by	Pierre Féménias (ESA)

CHRONOLOGY ISSUES

Issue	Date	Object
1.0	17/05/22	Draft version for Phase 2 PM#1
2.0	02/12/22	Intermediate version for Phase 2 PM #1 (80% completed for ENVISAT)
3.0	02/05/23	Final version for Final Review
4.0	23/05/23	Final version for Final Review with RIDs implemented
4.1	04/07/23	Final version for Final Review with RIDs implemented + document splitted

TABLE OF CONTENT

1	INTRODUCTION	5
1.1	THE FDR4ALT PROJECT	5
1.2	PURPOSE AND SCOPE OF THE VALIDATION REPORT	5
2	TERMINOLOGY	5
3	ATMOSPHERE THEMATIC DATA PRODUCTS	6
3.1	INTRODUCTION	6
3.2	VALIDATION APPROACH	6
3.3	VALIDATION DATASETS	7
3.3.1	<i>Parameters and characteristics</i>	7
3.3.2	<i>Product availability</i>	7
3.3.3	<i>Filtering</i>	7
3.4	VALIDATION RESULTS	8
3.4.1	<i>ERS-1</i>	8
3.4.2	<i>ERS-2</i>	12
3.4.3	<i>ENVISAT</i>	17
3.4.4	<i>Summary</i>	24
3.4.5	<i>Reference documents</i>	26
3.5	DIFFERENCE OF VARIANCE OF SSH AT CROSSOVER POINTS	26
3.5.1	<i>ENVISAT</i>	27
3.5.2	<i>ERS-2</i>	28
3.5.3	<i>ERS-1</i>	30
3.6	CONCLUSION AND REMARKS	31
	APPENDIX A - FDR4ALT DELIVERABLES	32

LIST OF FIGURES

FIGURE 3-1 – ERS-1: DAILY GLOBAL AVERAGE MONITORING OF THE WTC RETRIEVED FROM THE NN (ORANGE) OR THE 1DVAR (BLUE) APPROACH (LEFT) AND THE DIFFERENCES BETWEEN THE TWO APPROACHES (RIGHT). A 30-DAYS MOVING AVERAGE IS APPLIED TO SMOOTH THE DAILY DIFFERENCES. 9

FIGURE 3-2 –ERS-1: GEOGRAPHICAL DISTRIBUTION OF THE DIFFERENCES BETWEEN NN AND 1DVAR WTC (2°x2° GRIDDING AVERAGE OVER THE WHOLE VALIDATION PERIOD). 9

FIGURE 3-3 – ERS-1. ZONAL AVERAGES TCWV RETRIEVALS FROM OPERA (RED), 1DVAR (BLUE), AND ERA-5 (GREY) ON 11 APRIL 1996. 10

FIGURE 3-4 – ERS-1. TWO-DIMENSIONAL HISTOGRAMS COMPARING TCWV RETRIEVAL BETWEEN OPERA AND ERA-5 (LEFT) AS WELL AS 1DVAR AND ERA-5 (RIGHT) FOR 11 APRIL 1996. 10

FIGURE 3-5 – ERS-1: DAILY GLOBAL AVERAGE MONITORING OF THE ATMOSPHERIC ATTENUATION AT KU-BAND RETRIEVED FROM THE NN (ORANGE) OR THE 1DVAR (BLUE) APPROACH (LEFT) AND THE DIFFERENCES BETWEEN THE TWO APPROACHES (RIGHT). A 30-DAYS MOVING AVERAGE IS APPLIED TO SMOOTH THE DAILY DIFFERENCES..... 11

FIGURE 3-6 – ERS-1: GEOGRAPHICAL DISTRIBUTION OF THE DIFFERENCES BETWEEN NN AND 1DVAR ATT_KU (2°x2° GRIDDING AVERAGE OVER THE WHOLE VALIDATION PERIOD). 11

FIGURE 3-7 – ERS-1. LEFT: ZONAL AVERAGES OF OPERA (RED) AND 1DVAR (BLUE) LWP RETRIEVALS FOR 11 APRIL 1996. RIGHT: TWO-DIMENSIONAL HISTOGRAMS COMPARING INDIVIDUAL LWP RETRIEVALS FROM OPERA AND 1DVAR FOR THE SAME PERIOD. 12

FIGURE 3-8 – ERS-1. LEFT: HISTOGRAM OF OPERA LWP FOR 11 APRIL 1996. RIGHT: SAME FOR 1DVAR LWP. 12

FIGURE 3-9 – ERS-2: DAILY GLOBAL AVERAGE MONITORING OF THE WTC RETRIEVED FROM THE NN (ORANGE) OR THE 1DVAR (BLUE) APPROACH (LEFT) AND THE DIFFERENCES BETWEEN THE TWO APPROACHES (RIGHT). A 30-DAYS MOVING AVERAGE IS APPLIED TO SMOOTH THE DAILY DIFFERENCES. 13

FIGURE 3-10 –ERS-2: GEOGRAPHICAL DISTRIBUTION OF THE DIFFERENCES BETWEEN NN AND 1DVAR WTC (2°x2° GRIDDING AVERAGE OVER THE WHOLE VALIDATION PERIOD). 14

FIGURE 3-11 – ERS-2. ZONAL AVERAGES TCWV RETRIEVALS FROM OPERA (RED), 1DVAR (BLUE), AND ERA-5 (GREY) ON 11 APRIL 1996. 14

FIGURE 3-12 – ERS-2. TWO-DIMENSIONAL HISTOGRAMS COMPARING TCWV RETRIEVAL BETWEEN OPERA AND ERA-5 (LEFT) AS WELL AS 1DVAR AND ERA-5 (RIGHT) FOR 11 APRIL 1996. 15

FIGURE 3-13 – ERS-1: DAILY GLOBAL AVERAGE MONITORING OF THE ATMOSPHERIC ATTENUATION AT KU-BAND RETRIEVED FROM THE NN (ORANGE) OR THE 1DVAR (BLUE) APPROACH (LEFT) AND THE DIFFERENCES BETWEEN THE TWO APPROACHES (RIGHT). A 30-DAYS MOVING AVERAGE IS APPLIED TO SMOOTH THE DAILY DIFFERENCES..... 15

FIGURE 3-14 – ERS-2: GEOGRAPHICAL DISTRIBUTION OF THE DIFFERENCES BETWEEN NN AND 1DVAR ATT_KU (2°x2° GRIDDING AVERAGE OVER THE WHOLE VALIDATION PERIOD). 16

FIGURE 3-15 – ERS-2. LEFT: ZONAL AVERAGES OF OPERA (RED) AND 1DVAR (BLUE) LWP RETRIEVALS FOR 11 APRIL 1996. RIGHT: TWO-DIMENSIONAL HISTOGRAMS COMPARING INDIVIDUAL LWP RETRIEVALS FROM OPERA AND 1DVAR FOR THE SAME PERIOD. 16

FIGURE 3-16 – ERS-2. LEFT: HISTOGRAM OF OPERA LWP FOR 11 APRIL 1996. RIGHT: SAME FOR 1DVAR LWP. 17

FIGURE 3-17 – ENVISAT: DAILY GLOBAL AVERAGE MONITORING OF THE WTC RETRIEVED FROM THE NN (ORANGE) OR THE 1DVAR (BLUE) APPROACH (LEFT) AND THE DIFFERENCES BETWEEN THE TWO APPROACHES (RIGHT). A 30-DAYS MOVING AVERAGE IS APPLIED TO SMOOTH THE DAILY DIFFERENCES. 18

FIGURE 3-18 –ENVISAT: GEOGRAPHICAL DISTRIBUTION OF THE DIFFERENCES BETWEEN NN AND 1DVAR WTC (2°x2° GRIDDING AVERAGE OVER THE WHOLE VALIDATION PERIOD). 18

FIGURE 3-19 –SENTINEL-3A: GEOGRAPHICAL DISTRIBUTION OF THE DIFFERENCES BETWEEN NN AND 1DVAR WTC (4°x4° GRIDDING AVERAGE OVER 4 YEARS) [SOURCE: AMTROC STUDY FUNDED BY EUMETSAT]..... 19

FIGURE 3-20 –ENVISAT: MONITORING OF DIFFERENCE OF SSH VARIANCE BETWEEN N AND 1DVAR APPROACH (LEFT) AND GEOGRAPHICAL DISTRIBUTION OF THE DIFFERENCE(RIGHT). NEGATIVE VALUES: 1DVAR PERFORMS BETTER THAN NN, POSITIVE VALUES: OPERA PERFORMS BETTER THAN 1DVAR..... 19

FIGURE 3-21 –SENTINEL-3: MONITORING OF DIFFERENCE OF SSH VARIANCE BETWEEN 1DVAR AND NN APPROACH (LEFT) AND GEOGRAPHICAL DISTRIBUTION OF THE DIFFERENCE(RIGHT). NEGATIVE VALUES: 1DVAR PERFORMS BETTER THAN NN, POSITIVE VALUES: OPERA PERFORMS BETTER THAN 1DVAR..... 20



FIGURE 3-22 – ENVISAT: ZONAL AVERAGES OF 1DVAR (BLUE), OPERA (RED), AND ERA-5 (GREY) TCWV RETRIEVALS IN THE NORTHERN WINTER (LEFT, 6.-7. FEB. 2003, CYCLE 013, ORBITS 0662-0712) AND NORTHERN SUMMER (RIGHT, 16. AUG. 2002, CYCLE 008, ORBITS 0691-0719)..... 20

FIGURE 3-23 – ENVISAT: TWO-DIMENSIONAL HISTOGRAMS COMPARING THE TCWV RETRIEVAL OCCURRENCES BETWEEN 1DVAR AND ERA-5 (LEFT) AS WELL AS OPERA AND ERA-5 (RIGHT) FOR 23 JULY 2002 (CYCLE 008, ORBITS 0003-0032). 21

FIGURE 3-24 – ENVISAT. LEFT: 1DVAR TCWV ALONG ENVISAT CYCLE 008, ORBIT 0004 (23. JULY 2002) PROJECTED ON A MAP. RIGHT: COMPARISON OF 1DVAR (BLUE), OPERA (RED), AND ERA-5 (GREY) TCWV VALUES ALONG THE ORBIT SHOWN IN THE LEFT PANEL. . 21

FIGURE 3-25 – ENVISAT: DAILY GLOBAL AVERAGE MONITORING OF THE ATMOSPHERIC ATTENUATION AT KU-BAND RETRIEVED FROM THE NN (ORANGE) OR THE 1DVAR (BLUE) APPROACH (LEFT) AND THE DIFFERENCES BETWEEN THE TWO APPROACHES (RIGHT). A 30-DAYS MOVING AVERAGE IS APPLIED TO SMOOTH THE DAILY DIFFERENCES..... 22

FIGURE 3-26 – ENVISAT: GEOGRAPHICAL DISTRIBUTION OF THE DIFFERENCES BETWEEN NN AND 1DVAR ATT_KU (2°x2° GRIDDING AVERAGE OVER THE WHOLE VALIDATION PERIOD). 22

FIGURE 3-27 – ENVISAT. LEFT: ZONAL AVERAGES OF 1DVAR (BLUE) AND OPERA (RED) LWP RETRIEVALS IN THE NORTHERN WINTER (LEFT, 6.-7. FEB. 2003, CYCLE 013, ORBITS 0662-0712. RIGHT: TWO-DIMENSIONAL HISTOGRAMS COMPARING THE LWP RETRIEVAL OCCURRENCES BETWEEN 1DVAR AND OPERA FOR THE SAME PERIOD..... 23

FIGURE 3-28 – ENVISAT. LEFT: HISTOGRAM OF OPERA LWP FOR CYCLE 13 (13.1.- 17.2. 2003). RIGHT: SAME FOR 1DVAR LWP..... 24

FIGURE 3-29 – ENVISAT. LEFT: 1DVAR LWP ALONG ENVISAT CYCLE 008, ORBIT 0004 (23. JULY 2002) PROJECTED ON A MAP. RIGHT: COMPARISON OF OPERA (RED) AND 1DVAR (BLUE) LWP VALUES ALONG THE ORBIT SHOWN IN THE LEFT PANEL 24

FIGURE 3-30: ENVISAT : FMR V3 vs ANN ANALYSIS BY DIFFERENCE OF VARIANCE OF SSH AT CROSSOVER POINTS 27

FIGURE 3-31: ENVISAT : FMR V3 vs 1DVAR ANALYSIS BY DIFFERENCE OF VARIANCE OF SSH AT CROSSOVER POINTS..... 28

FIGURE 3-32: ENVISAT: 1DVAR vs ANN ANALYSIS BY DIFFERENCE OF VARIANCE OF SSH AT CROSSOVER POINTS 28

FIGURE 3-33: ERS-2: REAPER vs ANN ANALYSIS DIFFERENCE OF VARIANCE OF SSH AT CROSSOVER POINTS..... 29

FIGURE 3-34: ERS-2: REAPER vs 1DVAR ANALYSIS BY DIFFERENCE OF VARIANCE OF SSH AT CROSSOVER POINTS 29

FIGURE 3-35: ERS-2: 1DVAR vs ANN DIFFERENCE OF VARIANCE OF SSH AT CROSSOVER POINTS 30

FIGURE 3-36: ERS-1 : REAPER vs ANN DIFFERENCE OF VARIANCE OF SSH AT CROSSOVER POINTS 30

FIGURE 3-37: ERS-1: REAPER vs 1DVAR DIFFERENCE OF VARIANCE OF SSH AT CROSSOVER POINTS 31

FIGURE 3-38: ERS-1: 1DVAR vs ANN DIFFERENCE OF VARIANCE OF SSH AT CROSSOVER POINTS 31

LIST OF TABLES

TABLE 1 – SELECTED RETRIEVAL ASSESSMENT PARAMETERS FOR THE ATMOSPHERIC TDP AS OBTAINED FROM THE SPECIFIC VALIDATION CASES PRESENTED HEREIN 24

TABLE 2 : LIST OF FDR4ALT DELIVERABLES 32



1 Introduction

This document has been written in the frame of the FDR4ALT project, ESA contract N°4000128220/19/I-BG. It is a deliverable of task 4 of the project and is identified as [D-4-02].

1.1 The FDR4ALT Project

In the framework of the European Long Term Data Preservation Program (LTDP+) which aims at generating innovative Earth system data records named Fundamental Data Records (basically level 1 altimeter and radiometer data) and Thematic Data Records (basically level 2+ geophysical products), ESA/ESRIN has launched a reprocessing activity of ERS-1, ERS-2 and ENVISAT altimeter and radiometer dataset, called the FDR4ALT project (Fundamental Data Records for Altimetry). A large consortium of thematic experts has been formed to perform these activities which are:

- 1) To define products including the long, harmonized record of uncertainty-quantified observations.
- 2) To define the most appropriate level 1 and level 2 processing.
- 3) To reprocess the whole times series according to the predefined processing.
- 4) To validate the different products and provide them to large communities of users focused on the observation of the atmosphere, ocean topography, ocean waves, coastal, hydrology, sea ice, ice sheet regions.

1.2 Purpose and scope of the validation report

After the FDR/TDP definition step and all benchmarking (Round Robin) between standard solutions addressed by each expert group, comes the production and validation step.

The objective of this document is to provide a validation report for the Atmosphere TDP, following the strategy defined in the Validation Plan Document [D-4-01]. Note that to avoid heavy documents, the validation reports have been divided: there is one validation report for the FDRs (ALT FDR and MWR FDR) and one validation for each of the six TDPs. This document therefore contains only results for the **Atmosphere TDP**.

This document describes in detail the validation that has been performed for the Sea-Ice TDP to assess the performances of the FDR4ALT final products. The validation covers the full lifespan of the missions and therefore includes long-term analysis, as well as cyclic analysis or targeted analysis that are relevant for this TDP.

2 Terminology

This section aims at defining clearly the terminology used in the FDR4ALT deliverables.

- **Product** refers a specific type of file, defined and described by a dedicated handbook, and designed for a clear purpose (the FDR4ALT project, the REAPER project, ...). It is a “container”. One product refers to one file. The use of plural is designed to refer to a group of files, for instance the Thematic Data Products. “FDR4ALT products” will usually refer to all TDPs and FDRs, i.e., the outputs of the whole project. Note that the word “product” does not imply any notion of start date or end date, whereas “dataset” does.
- **File** can be used to refer to one single product or any other file that is not a product.

- **Parameter or variable** refers to a product’s field, i.e., the content of the product. For instance, the sea level anomaly is a parameter of the Ocean & Coastal Thematic Data Products.
Dataset can be used to refer to any group of data, not necessarily products. However, in the context of this project, it will often be used to refer to a sub-ensemble of products, on a specific period of time or a specific geographic area. For instance, the TDS (test dataset) refers to a dataset of 3 years of test products.

3 Atmosphere Thematic Data Products

3.1 Introduction

The Atmospheric TDP produced in the context of the FDR4ALT project comprise *Total Column Water Vapour* (TCWV), *Cloud Liquid Water Path* (LWP), *Atmospheric Attenuation* of the altimeter backscattering coefficient (AttKu), and *Wet Tropospheric Correction* (WTC) retrieved from observations of the Microwave Radiometer (MWR) instruments flown on-board the ERS-1, and ERS-2, and ENVISAT satellites.

The FDR4ALT Atmospheric TDP is produced using two different processing streams: the standard operational products (“OPERA”) are derived using a neural network approach and distributed through the “main” group of the FDR4ALT Atmospheric TDP product files. Additionally, 1DVAR based retrievals are provided through the “expert” group of the Atmospheric TDP.

The aim of this validation exercise is to identify strengths and weaknesses of both the OPERA and the 1DVAR Atmospheric TDP retrieval schemes, and to such provide interested users with the information needed to make well-informed decisions about the potential uptake of FDR4ALT atmospheric products. In addition, leads towards further retrieval improvements shall be identified.

3.2 Validation approach

Each Atmospheric TDP parameter will be validated with a dedicated approach since the availability of reference data differs. Most emphasis is put on TCWV which is an Essential Climate Variable (ECV) in its own right, and WTC considering its importance for altimetry.

The validation of the atmospheric TDP parameters needs to account for the limited availability of independent reference data from, e.g., operational radiosonde or GNSS networks, since only MWR observations located at least 50 km offshore are being validated to avoid land contamination. Herein, we therefore compare the operational ANN-based OPERA “main” products as well as the 1DVAR “expert” products against the corresponding ERA-5 values. Additionally, individual orbits are analysed to identify specific situations where OPERA and 1DVAR retrievals significantly diverge with the aim to identify the potential underlying causes.

The validation strategy pursued herein is to focus on selected target areas and/or time periods that allow for the analysis of retrieval performance with respect to specific regional, zonal, seasonal, or multi-annual patterns and processes.

Target areas:

- Large scale areas over the global ice-free open ocean have been used to provide retrieval statistics between corresponding satellite-derived products.
- Regional areas have been identified to perform detailed analyses of retrieval performance under conditions potentially influencing retrieval quality have (e.g., wet vs. dry atmospheres, high vs. low wind speed, ...).

- To avoid contamination by land, only retrievals located at least 50 km offshore have been considered.

Target periods:

- Depending on the specific aspect to be investigated, chosen target periods encompass a single orbit, one full day (i.e., ca. 14 full orbits), one full cycle (ca. 35 days), or longer periods to study seasonal or inter-annual trends.

3.3 Validation datasets

3.3.1 Parameters and characteristics

The validation of the Atmospheric TDP is based on the following datasets:

- Atmospheric TDP parameters (TCWV, WTC, LWP, ATT_KU) from FDR4ALT processing:
 - Main group: “OPERA” results, retrieved using a Neural Network approach.
 - Expert group: “1DVAR” results, retrieved from a one-dimensional variational approach.
- Corresponding ERA-5 reanalysis (TCWV only).

Atmospheric TDP is calculated from 7 Hz MWR FDR. No temporal averaging is applied, so that the resulting L2 products are also available at 7 Hz temporal resolution.

3.3.2 Product availability

For every MWR FDR L1B data file (representing half of an orbit), a corresponding L2 file has been generated (but see the note below). The formal spatial and temporal coverage of the Atmospheric TDP is thus equivalent to the availability of the underlying MWR L1B FDR (see the Product Validation Report (FDR) for details). However, actual availability of valid L2 products is lower since Atmospheric TDP have only been derived for the ice-free global oceans. Retrieval is also impossible under specific meteorological conditions, e.g., heavy precipitation, further reducing L2 product availability.

Note that the availability of 1DVAR products is slightly reduced as compared to that of the corresponding OPERA products. This is because a limited number of L1B input files were not available when producing 1DVAR L2 products while they were available at a later stage when producing the OPERA L2 products. The reasons discrepancy for this are not fully clear yet – but interestingly, the earlier not available L1B files all correspond to orbits starting between 18:00 and 23:00 UTC. Since this discrepancy was only noted late in the project when merging the OPERA and 1DVAR final L2 products, it was not possible to generate the missing 1DVAR products within the remaining project delays. Consequently, there are a number of orbits containing only OPERA L2, but not the corresponding 1DVAR L2 products. Fortunately, the amount of missing 1DVAR products is rather low (less than 2% of the total amount of L2 products) as specified below in the “Completeness” sections for each instrument.

3.3.3 Filtering

The 1DVAR L2 product comes with a validity flag that allows for the identification of missing or questionable retrievals. The flagging philosophy is different for the OPERA products where users have to apply their own use-case specific flagging.

Observations suitable for validation have been identified herein through the following criteria which ALL must be met:

- 1DVAR validity flag equals 0 (i.e., 1DVAR retrieval has been successful) AND

- OPERA retrieval exists (i.e., an OPERA value is available) AND
- Distance from coast > 50 km AND
- ERA-5 TCWV exists (only applicable to TCWV validation).

3.4 Validation results

Validation results are shown separately for ERS-1, ERS-2, and ENVISAT. Most effort has been put into the validation of ENVISAT retrievals, for that practical reason that the ENVISAT products were available first so that more time could be spent on assessing their quality.

3.4.1 ERS-1

3.4.1.1 Completeness

Number of processed L1B files: 49,067.

Number of OPERA L2 files: 49,067.

Number of 1DVAR L2 files: 48,202 (equiv. ca. 1.8 % product reduction).

3.4.1.2 Wet tropospheric correction

The wet tropospheric correction is validated over the tandem phase period with ERS-2, from 17/08/1995 to 02/06/1996 (cycle 148 to cycle 156). Retrievals located at latitudes higher than 50° are edited in order to mitigate the impact of ice contamination.

The daily global average monitoring of the WTC (see Figure 3-1, left) shows consistent results between OPERA/NN (orange) and 1DVAR (blue) approaches with a stable bias of about 2.5 mm between the two (see Figure 3-1, right). This is very similar to what is observed over the same period for ERS-2 but slightly smaller than what is observed on ENVISAT (see the corresponding following paragraphs).

The high consistency between NN and 1DVAR at global scale actually hides a more contrasted regional distribution of the differences between NN and 1DVAR WTC as shown in Figure 3-2, representing the geographical distribution of the NN-1DVAR WTC difference for 2°x2° averages over the whole validation period. This difference clearly exhibits two modes. The first mode over the tropics (latitudes between -30° and +30°) is characterized by a 1DVAR WTC wetter than the NN WTC by a few millimeters over the clear-sky regions up to 1 to 2 cm over the wetter areas (Indo-pacific warm pool region for instance). The second mode at higher latitudes is characterized by a NN WTC wetter than the 1DVAR WTC by about 0.2 cm. Again, this is very similar to what is observed over the same period for ERS-2 but slightly smaller than what is observed on ENVISAT (see the corresponding following paragraphs).

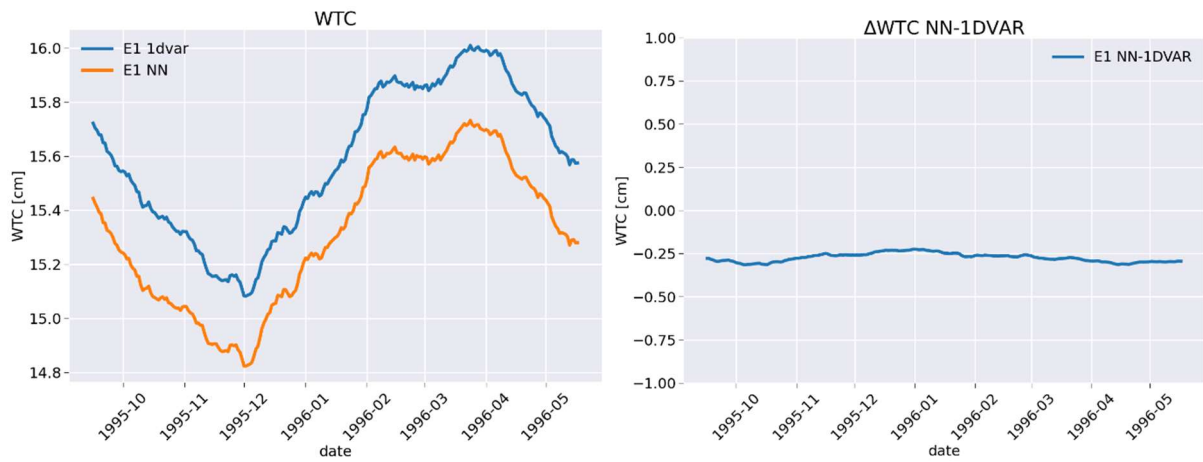


Figure 3-1 – ERS-1: Daily global average monitoring of the WTC retrieved from the NN (orange) or the 1DVAR (blue) approach (left) and the differences between the two approaches (right). A 30-days moving average is applied to smooth the daily differences.

These differences are not fully understood yet. Potential explanations could be attributed to a difference in the bias corrections of the observed TB at the input of the retrieval or specific sensitivity of either retrieval to the prevailing geophysical conditions (water vapor, surface roughness, precipitation). While it is difficult to disentangle the source of the differences, it is worth noting that:

- 1- The biases are somehow related to the geographical pattern of the variance of SSH metric.
- 2- The results are consistent (yet with a different distribution) with the equivalent analysis performed for the Sentinel-3A and -3B missions (Figure 3-12).

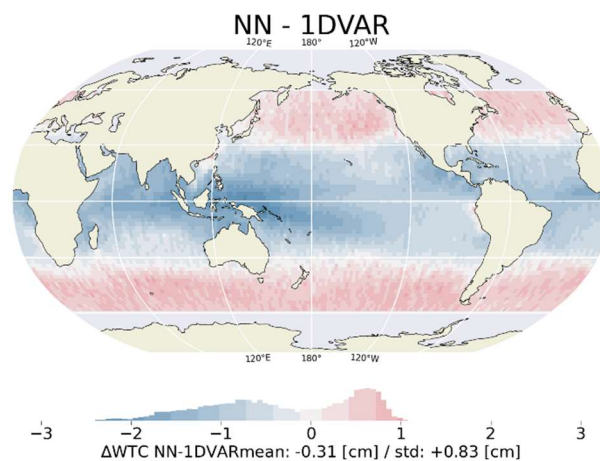


Figure 3-2 – ERS-1: Geographical distribution of the differences between NN and 1DVAR WTC ($2^\circ \times 2^\circ$ gridding average over the whole validation period).

3.4.1.3 Total column water vapour

Figure 3-3 shows the zonal averages of ERS-1 TCWV from OPERA, 1DVAR, and ERA-5 for latitudinal zones of five degrees extension for 11 April 1996. While there is rather good agreement between all three products within the TCWV range of ca. 15-30 kg/m², 1DVAR and ERA-5 show increasingly higher TCWV values than OPERA above ca. 30 kg/m². In the tropics, where the highest zonally averaged TCWV values are encountered, the TCWV difference 1DVAR/ERA-5 – OPERA amounts to ca. 5 kg/m². This picture somewhat reverses for TCWV concentrations < 10 kg/m², where 1DVAR shows on average lower values than OPERA and ERA-5.

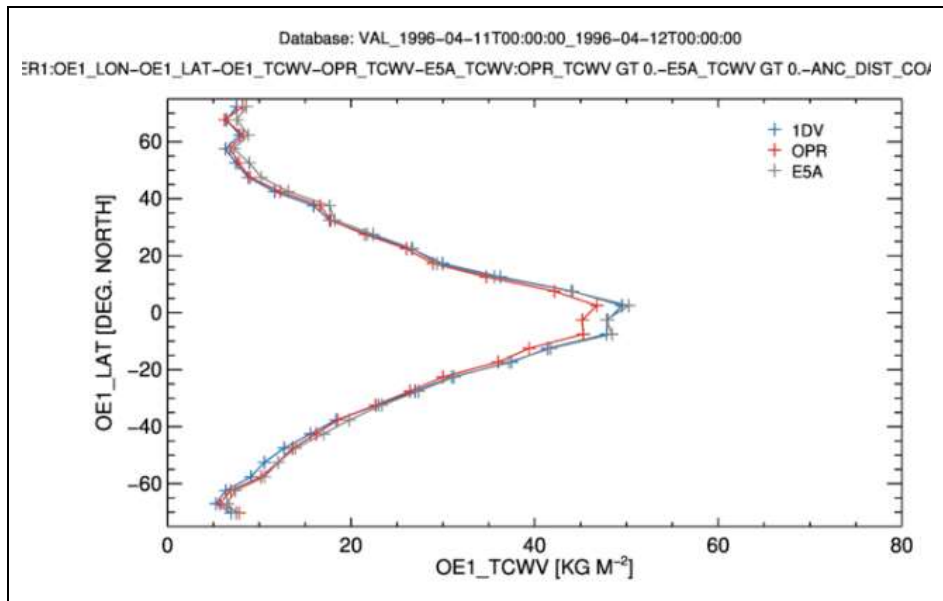


Figure 3-3 – ERS-1. Zonal averages TCWV retrievals from OPERA (red), 1DVAR (blue), and ERA-5 (grey) on 11 April 1996.

These principal differences are confirmed by the scattering plots shown in Figure 3-4 for the same period. OPERA is on average slightly drier than 1DVAR as compared to ERA-5 (TCWV bias of -1.11 kg/m^2 for OPERA and -0.74 kg/m^2 for 1DVAR). The wider TCWV range covered by 1DVAR as compared to OPERA results in differing offsets and slopes when compared against ERA-5, with a slope of 1.03 for OPERA (ERA-5 wetter) and a slope of 0.96 for 1DVAR (ERA-5 drier). The correlation coefficients are almost identical with $r=0.979$ for OPERA vs. ERA-5 and $r=0.983$ for 1DVAR vs. ERA-5.

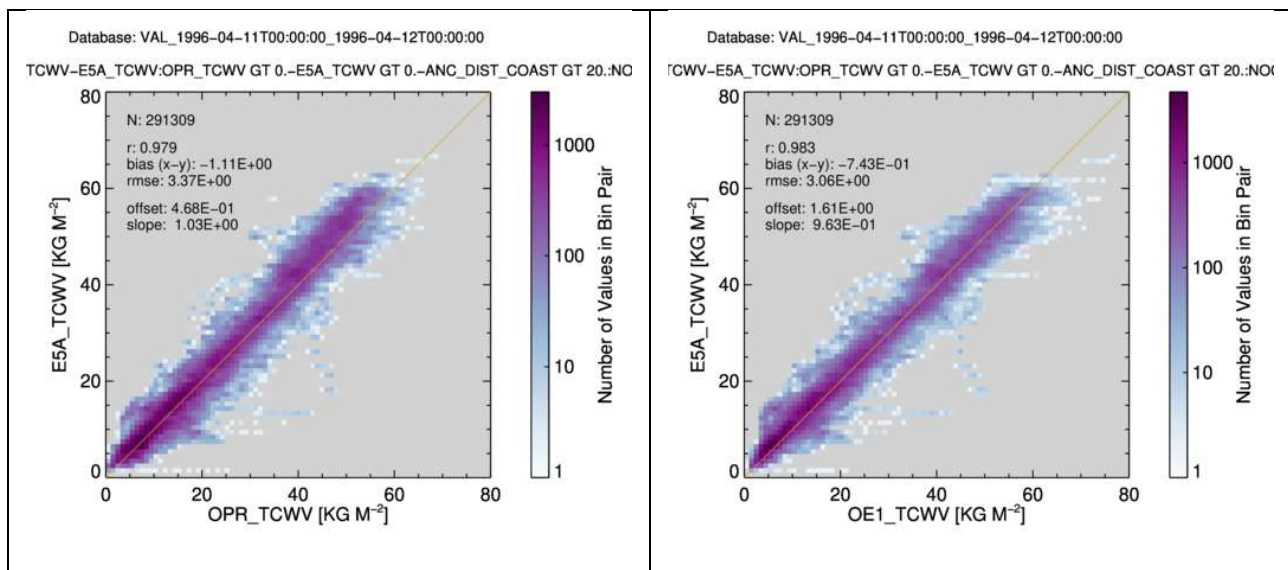


Figure 3-4 – ERS-1. Two-dimensional histograms comparing TCWV retrieval between OPERA and ERA-5 (left) as well as 1DVAR and ERA-5 (right) for 11 April 1996.

3.4.1.4 Atmospheric attenuation at Ku-band

Atmospheric attenuation at Ku-band (ATT_KU in the following) is validated over the tandem phase period with ERS-2, from 17/08/1995 to 02/06/1996 (cycle 148 to cycle 156). Retrievals located at latitudes higher than 50° are edited in order to mitigate the impact of ice contamination.

The daily global average monitoring of the ATT_KU (see Figure 3-5 Figure , left) enables the comparison between NN (orange) and 1DVAR (blue) approaches. A bias of about 0.035 dB is observed between the two retrievals (Figure , right), with higher values for the NN.

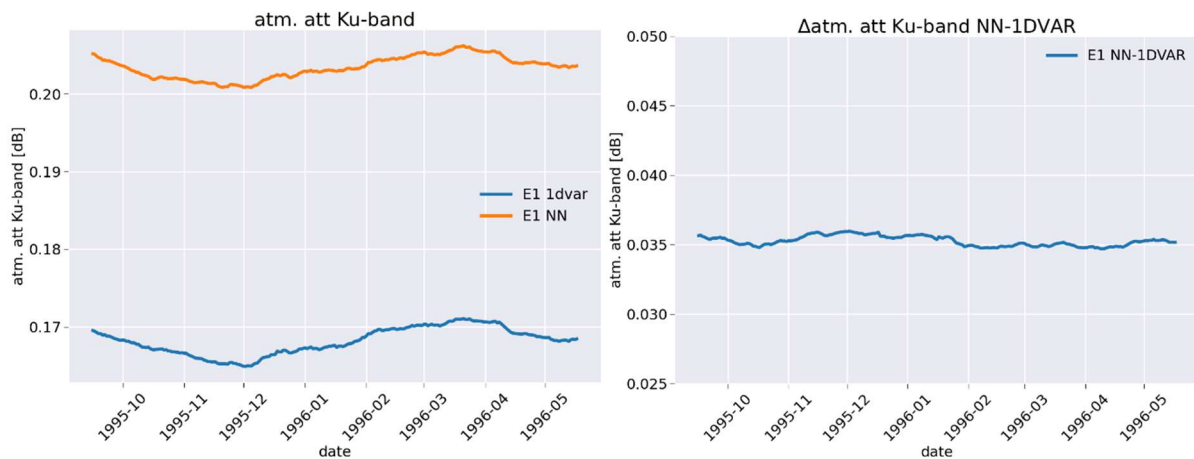


Figure 3-5 – ERS-1: Daily global average monitoring of the atmospheric attenuation at Ku-band retrieved from the NN (orange) or the 1DVAR (blue) approach (left) and the differences between the two approaches (right). A 30-days moving average is applied to smooth the daily differences.

Figure 3-6 shows the geographical distribution of the differences between NN and 1DVAR ATT_KU (2°x2° gridding average over the whole validation period). Over wet regions located around the ITCZ (Inter Tropical Convergence Zone) the bias is small, below 0.02 dB, but larger over drier and high latitudes regions, reaching about 0.05 dB.

It is not possible for the moment to conclude which retrieval offers the better performance. In this respect, it would be interesting to compare the statistics of the retrievals against the expected values computed from a line-by-line or an empirical model to verify if one of the two solutions is closer to the theory.

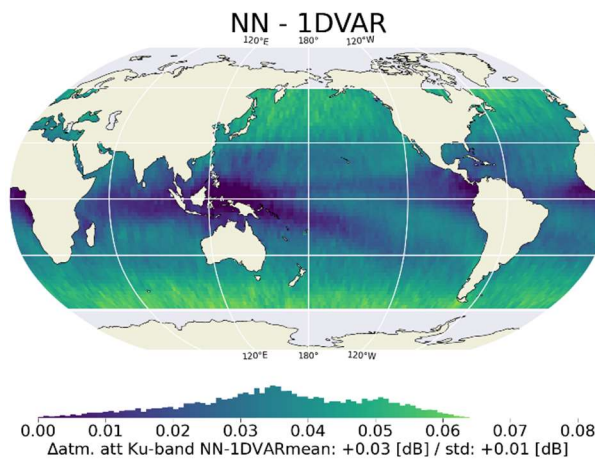


Figure 3-6 – ERS-1: Geographical distribution of the differences between NN and 1DVAR ATT_KU (2°x2° gridding average over the whole validation period).

3.4.1.5 Liquid water path

Figure 3-7 (left) shows averages of ERS-1 LWP from OPERA and 1DVAR for latitudinal zones of five degrees extension for 11 April 1996. While the two products show a highly correlated zonal LWP distribution, there is a wide gap in absolute LWP retrieval of ca. 0.07 – 0.10 kg/m² which appears to be widening with increasing LWP. The main reason for this gap lies in the fact that 1DVAR LWP retrievals are negatively biased (Figure 3-7, right), leading to negative LWP values in cloud-free areas, while OPERA LWP retrievals are positively

biased (Figure 3-7, left) and negative OPERA LWP retrievals are additionally set to 0.0 kg/m² leading to increased positive bias in cloud-free areas.

The enforced lower boundary at LWP = 0.0 kg/m² for OPERA retrievals is clearly visible in Figure 3-7 (right) which also confirms the good correlation ($r=0.942$) and the large bias (1DVAR-OPERA = -0.087 kg/m²) between the two retrievals.

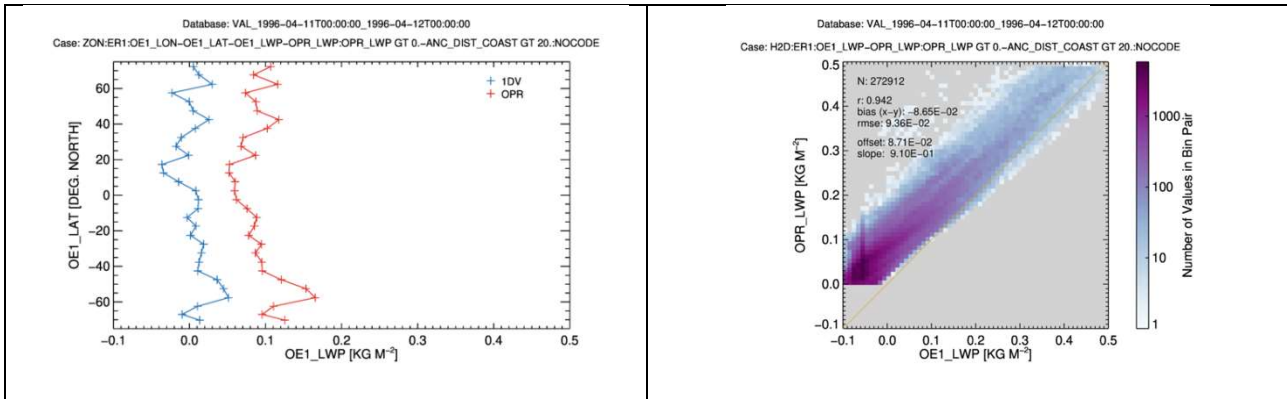


Figure 3-7 – ERS-1. Left: Zonal averages of OPERA (red) and 1DVAR (blue) LWP retrievals for 11 April 1996. Right: Two-dimensional histograms comparing individual LWP retrievals from OPERA and 1DVAR for the same period.

This is further illustrated in Figure 3-8 showing histograms of the ERS-1 LWP distribution for 11 April 1996. Since the cloud-free case is the most likely, the histograms should peak at LWP = 0.0 kg/m² with a retrieval-dependent scatter around this value. However, Figure 3-8 (left) shows that OPERA has a bias of at least +0.025 kg/m² (mode at +0.025 kg/m² plus the additionally increasing effect of forcing negative retrievals to zero). In contrast, 1DVAR has a negative bias of -0.055 kg/m² (Figure 3-8, right), resulting in the observed combined average difference LWP OPERA – LWP 1DVAR of ca. 0.080 - 0.090 kg/m²

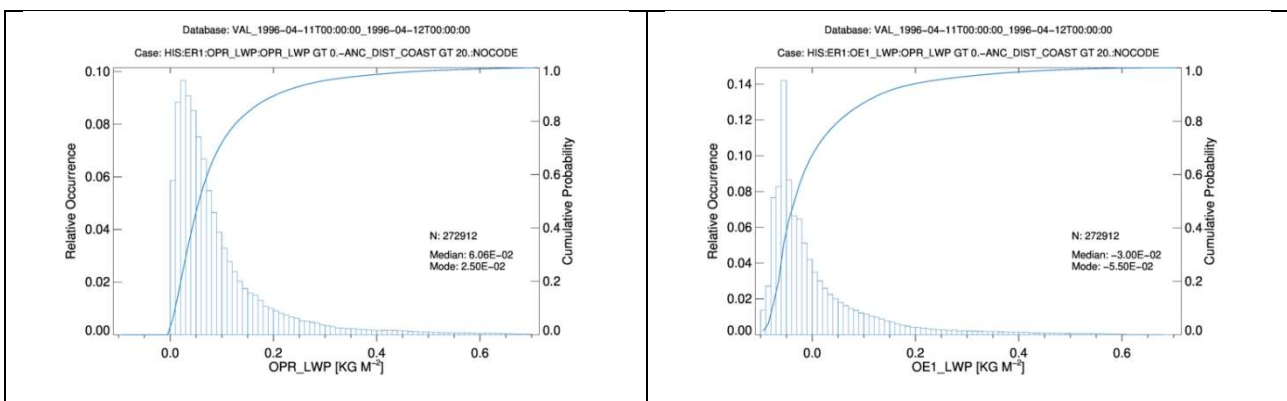


Figure 3-8 – ERS-1. Left: Histogram of OPERA LWP for 11 April 1996. Right: Same for 1DVAR LWP.

See Section 3.4.3.5 for further discussion on the LWP retrieval differences in OPERA and 1DVAR.

3.4.2 ERS-2

3.4.2.1 Completeness

Number of processed L1B files: 150,481.

Number of OPERA L2 files: 150,481.

Number of 1DVAR L2 files: 148,918 (equiv. ca. 1.0 % product reduction).

3.4.2.2 Wet tropospheric correction

The wet tropospheric correction is validated over the tandem phase period with ERS-1, from 17/08/1995 to 02/06/1996 (cycle 0 to cycle 12). Retrievals located at latitudes higher than 50° are edited in order to mitigate the impact of ice contamination.

The daily global average monitoring of the WTC (see Figure 3-9, left) shows consistent results between OPERA/NN (orange) and 1DVAR (blue) approaches with a stable bias of about 2.5 mm between the two (see Figure 3-9, right). This is very similar to what is observed over the same period for ERS-1 but slightly smaller than what is observed on ENVISAT (see the corresponding following paragraphs).

The high consistency between NN and 1DVAR at global scale actually hides a more contrasted regional distribution of the differences between NN and 1DVAR WTC as shown in Figure 3-10, representing the geographical distribution of the NN-1DVAR WTC difference for 2°x2° averages over the whole validation period. This difference clearly exhibits two modes. The first mode over the tropics (latitudes between -30° and +30°) is characterized by a 1DVAR WTC wetter than the NN WTC by a few millimeters over the clear-sky regions up to 1 to 2 cm over the wetter areas (Indo-pacific warm pool region for instance). The second mode at higher latitudes is characterized by a NN WTC wetter than the 1DVAR WTC by about 0.2 cm. Again, this is very similar to what is observed over the same period for ERS-1 but slightly smaller than what is observed on ENVISAT (see the corresponding following paragraphs).

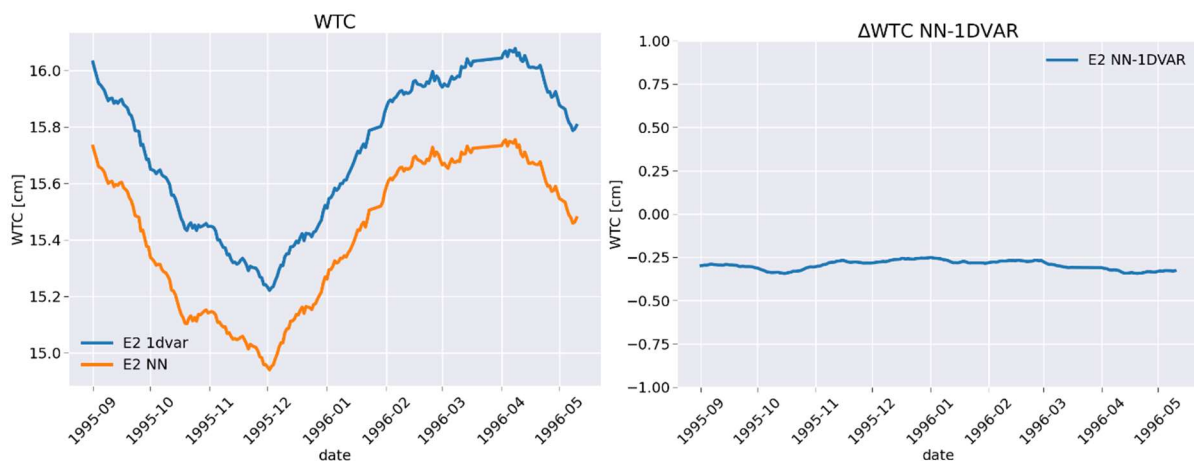


Figure 3-9 – ERS-2: Daily global average monitoring of the WTC retrieved from the NN (orange) or the 1DVAR (blue) approach (left) and the differences between the two approaches (right). A 30-days moving average is applied to smooth the daily differences.

These differences are not fully understood yet. Potential explanations could be attributed to a difference in the bias corrections of the observed TB at the input of the retrieval or specific sensitivity of either retrieval to the prevailing geophysical conditions (water vapor, surface roughness, precipitation). While it is difficult to disentangle the source of the differences, it is worth noting that:

- 3- The biases are somehow related to the geographical pattern of the variance of SSH metric.
- 4- The results are consistent (yet with a larger amplitude) with the equivalent analysis performed for the Sentinel-3A and -3B missions (Figure 3-19).

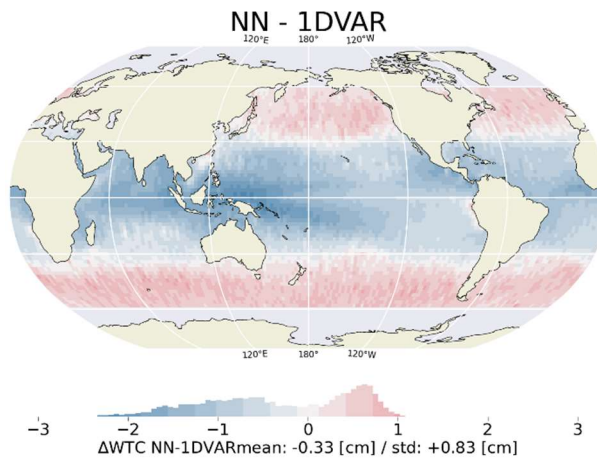


Figure 3-10 –ERS-2: Geographical distribution of the differences between NN and 1DVAR WTC ($2^\circ \times 2^\circ$ gridding average over the whole validation period).

3.4.2.3 Total column water vapour

Figure 3-11 shows averages of ERS-2 TCWV from OPERA, 1DVAR, and ERA-5 for latitudinal zones of five degrees extension for 11 April 1996, i.e., the same day used to assess TCWV retrieval performance for ERS-1 as shown in Figure 3-3. There are only minor differences between ERS-1 and ERS-2 TCWV retrievals: again, there is rather good agreement between all three products within the TCWV range of ca. 15-30 kg/m², 1DVAR and ERA-5 show increasingly higher TCWV values than OPERA above ca. 30 kg/m². In the tropics, where the highest zonally averaged TCWV values are encountered, the TCWV difference 1DVAR/ERA-5 – OPERA amounts to ca. 3 kg/m² (as compared to ca. 5 kg/m² for ERS-1). For TCWV concentrations < 10 kg/m², 1DVAR shows somewhat lower values than OPERA and even more so against ERA-5.

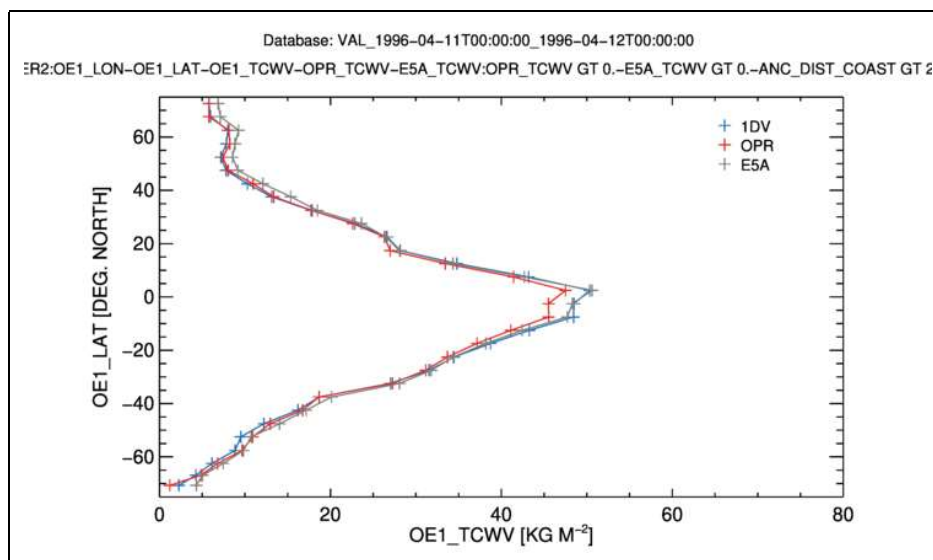


Figure 3-11 – ERS-2. Zonal averages TCWV retrievals from OPERA (red), 1DVAR (blue), and ERA-5 (grey) on 11 April 1996.

These principal differences are confirmed by the scattering plots shown in Figure 3-12 for the same period. OPERA is on average slightly drier than 1DVAR as compared to ERA-5 (TCWV bias of -1.07 kg/m² for OPERA and -0.61 kg/m² for 1DVAR). The wider TCWV range covered by 1DVAR as compared to OPERA results in differing offsets and slopes when compared against ERA-5, with a slope of 1.02 for OPERA (ERA-5 wetter) and a slope of 0.96 for 1DVAR (ERA-5 drier). The correlation coefficients are almost identical with $r=0.983$ for OPERA vs. ERA-5 and $r=0.986$ for 1DVAR vs. ERA-5.

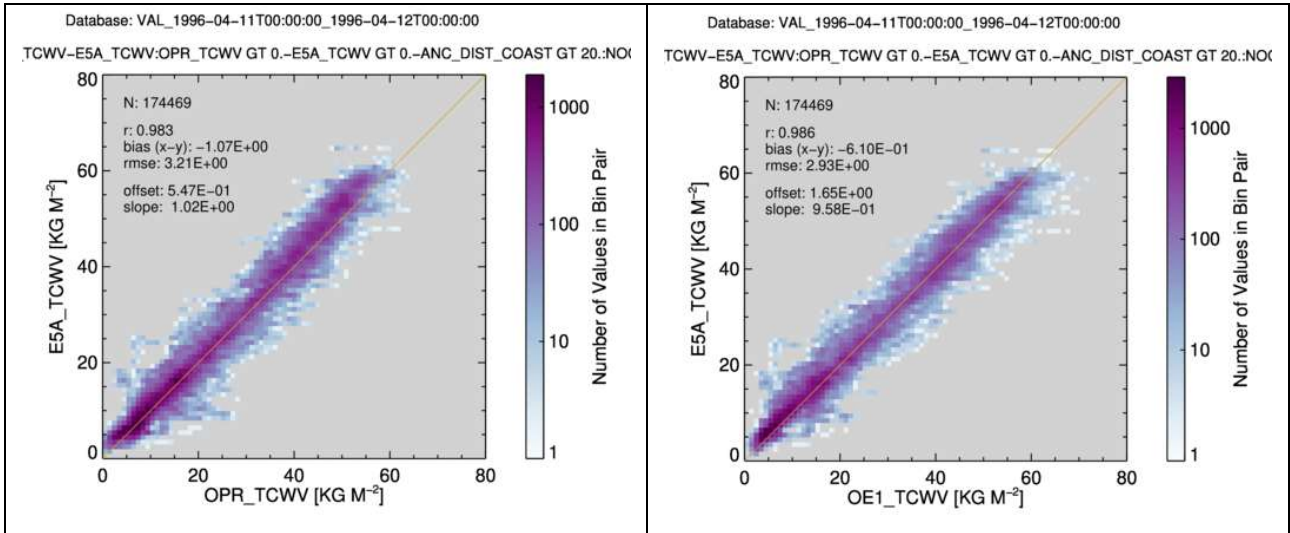


Figure 3-12 – ERS-2. Two-dimensional histograms comparing TCWV retrieval between OPERA and ERA-5 (left) as well as 1DVAR and ERA-5 (right) for 11 April 1996.

3.4.2.4 Atmospheric attenuation at Ku-band

Atmospheric attenuation at Ku-band (ATT_KU in the following) is validated over the tandem phase period with ERS-2, from 17/08/1995 to 02/06/1996 (cycle 148 to cycle 156). Retrievals located at latitudes higher than 50° are edited in order to mitigate the impact of ice contamination.

The daily global average monitoring of the ATT_KU (see Figure 3-13, left) enables the comparison between NN (orange) and 1DVAR (blue) approaches. A bias of about 0.035 dB is observed between the two retrievals (Figure 3-13,, right), with higher values for the NN.

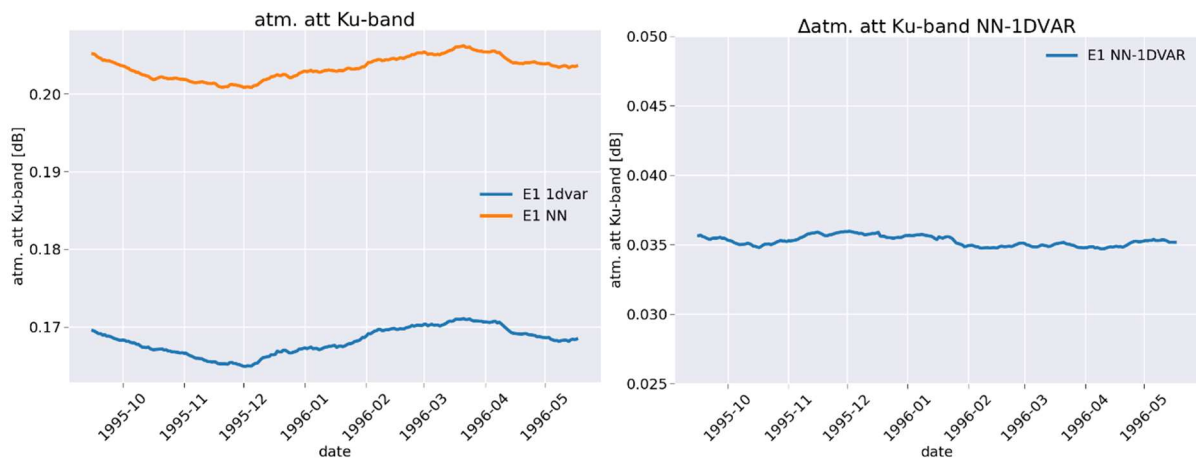


Figure 3-13 – ERS-1: Daily global average monitoring of the atmospheric attenuation at Ku-band retrieved from the NN (orange) or the 1DVAR (blue) approach (left) and the differences between the two approaches (right). A 30-days moving average is applied to smooth the daily differences.

Figure 3-14 shows the geographical distribution of the differences between NN and 1DVAR ATT_KU (2°x2° gridding average over the whole validation period). Over wet regions located around the ITCZ (Inter Tropical Convergence Zone) the bias is small, below 0.02 dB, but larger over drier and high latitudes regions, reaching about 0.05 dB.

It is not possible for the moment to conclude which retrieval offers the better performance. In this respect, it would be interesting to compare the statistics of the retrievals against the expected values computed from a line-by-line or an empirical model to verify if one of the two solutions is closer to the theory.

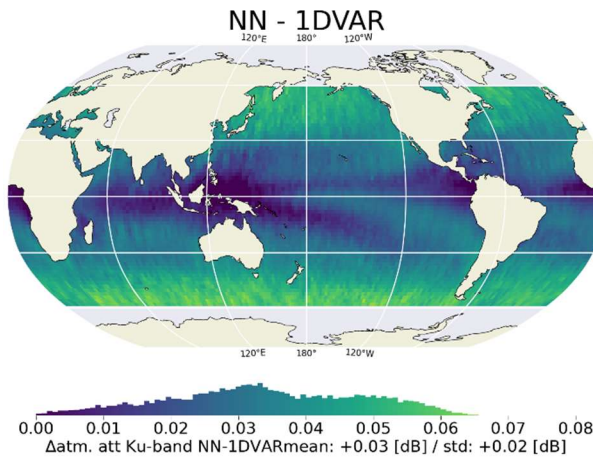


Figure 3-14 – ERS-2: Geographical distribution of the differences between NN and 1DVAR ATT_KU ($2^\circ \times 2^\circ$ gridding average over the whole validation period).

3.4.2.5 Liquid water path

Figure 3-15 (left) shows averages of ERS-2 LWP from OPERA and 1DVAR for latitudinal zones of five degrees extension for 11 April 1996. The conclusions drawn from the comparison of ERS-1 LWP retrievals do mostly also apply to ERS-2 LWP retrievals: both products show a highly correlated zonal LWP distribution with a wide gap in absolute LWP retrieval of ca. $0.07 - 0.10 \text{ kg/m}^2$ which appears to be widening with increasing LWP. The main reason for this gap lies in the fact that 1DVAR LWP retrievals are negatively biased (Figure 3-16, right), leading to negative LWP values in cloud-free areas, while OPERA LWP retrievals are positively biased (Figure 3-16, left) and negative OPERA LWP retrievals are set to 0.0 kg/m^2 leading to an additional positive bias in cloud-free areas.

The enforced lower boundary at $\text{LWP} = 0.0 \text{ kg/m}^2$ for OPERA retrievals is clearly visible in Figure 3-15 (right) which also confirms the rather good correlation ($r=0.920$, but slightly lower than for ERS-1 with $r=0.942$) and the almost identical bias of $1\text{DVAR-OPERA} = -0.085 \text{ kg/m}^2$ (as compared to -0.087 kg/m^2 for ERS-1) between the two retrievals.

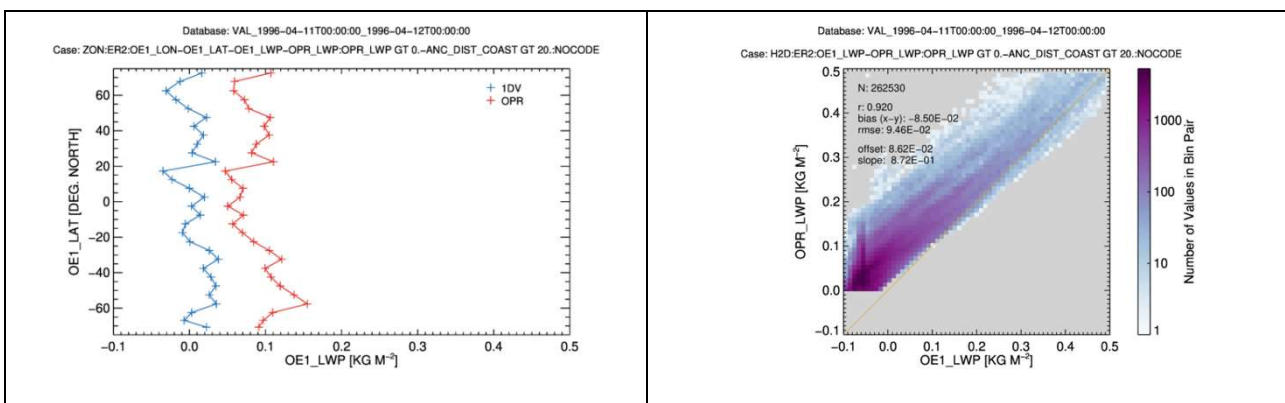


Figure 3-15 – ERS-2. Left: Zonal averages of OPERA (red) and 1DVAR (blue) LWP retrievals for 11 April 1996. Right: Two-dimensional histograms comparing individual LWP retrievals from OPERA and 1DVAR for the same period.

This is further illustrated in Figure 3-16 showing histograms of the ERS-2 LWP distribution for 11 April 1996. Since the cloud-free case is by far the most likely, the histograms should peak at $\text{LWP} = 0.0 \text{ kg/m}^2$ with a retrieval-dependent scatter around this value. However, Figure 3-16 (left) shows that OPERA has a bias of at

least $+0.025 \text{ kg/m}^2$ (mode at $+0.025 \text{ kg/m}^2$ plus additional increasing effect of forcing negative retrievals to zero). In contrast, 1DVAR has a negative bias of -0.055 kg/m^2 (Figure 3-16, right), resulting in the observed combined average difference LWP OPERA – LWP 1DVAR of ca. $0.080 - 0.090 \text{ kg/m}^2$.

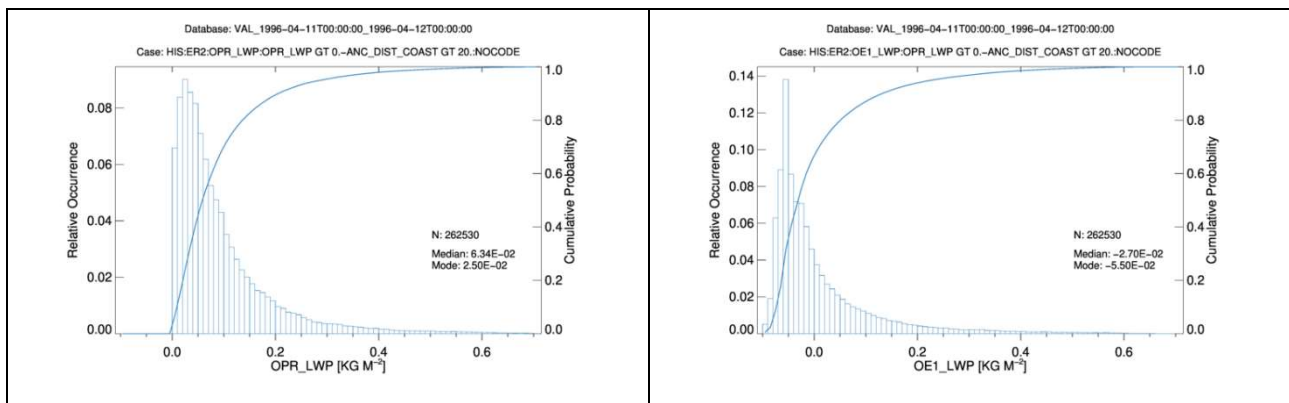


Figure 3-16 – ERS-2. Left: Histogram of OPERA LWP for 11 April 1996. Right: Same for 1DVAR LWP.

See Section 3.4.3.5 for further discussion on the LWP retrieval differences in OPERA and 1DVAR.

3.4.3 ENVISAT

3.4.3.1 Completeness

Number of processed L1B files: 101,154.

Number of OPERA L2 files: 101,154.

Number of 1DVAR L2 files: 99,361 (equiv. ca. 1.8 % product reduction).

3.4.3.2 Wet tropospheric correction

The wet tropospheric correction is validated over the period covered by cycle 8 to cycle 13. Retrievals located at latitudes higher than 50° are edited in order to mitigate the impact of ice contamination.

The daily global average monitoring of the WTC (see Figure 3-17, left) shows consistent results between OPERA/NN (orange) and 1DVAR (blue) approaches with a stable bias of about 3-4 mm between the two (see Figure 3-17, right). Note the small drop of about 1 mm for the NN approach occurring in the second half of August 2002 which is also observed on all the geophysical parameters. The reasons for this drop are not clear as of now, but should be further investigated.

The high consistency between NN and 1DVAR at global scale actually hides a more contrasted regional distribution of the differences between NN and 1DVAR WTC as shown in Figure 3-18, representing the geographical distribution of the NN-1DVAR WTC difference for $2^\circ \times 2^\circ$ averages over the whole validation period. This difference clearly exhibits two modes. The first mode over the tropics (latitudes between -30° and $+30^\circ$) is characterized by a 1DVAR WTC wetter than the NN WTC by less than 1 cm over the clear-sky regions up to 3 cm over the wetter areas (Indo-pacific warm pool region for instance). The second mode at higher latitudes is characterized by a NN WTC wetter than the 1DVAR WTC by about 0.5 cm.



Figure 3-17 – ENVISAT: Daily global average monitoring of the WTC retrieved from the NN (orange) or the 1DVAR (blue) approach (left) and the differences between the two approaches (right). A 30-days moving average is applied to smooth the daily differences.

These differences are not fully understood yet. Potential explanations could be attributed to a difference in the bias corrections of the observed TB at the input of the retrieval or specific sensitivity of either retrieval to the prevailing geophysical conditions (water vapor, surface roughness, precipitation). While it is difficult to disentangle the source of the differences, it is worth noting that:

- 5- The biases are somehow related to the geographical pattern of the variance of SSH metric.
- 6- The results are consistent (yet with a larger amplitude) with the equivalent analysis performed for the Sentinel-3A and -3B missions (Figure 3-19).

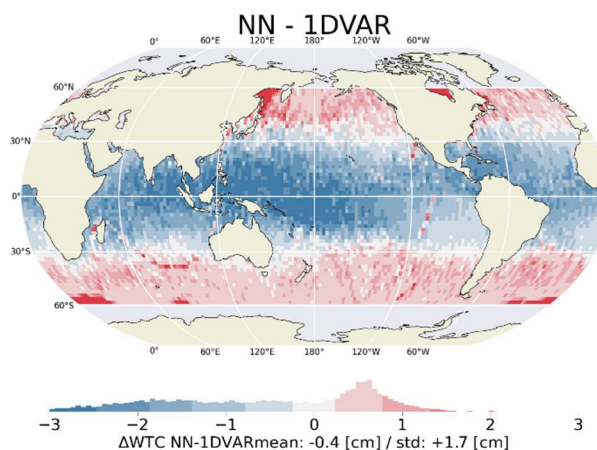


Figure 3-18 – ENVISAT: Geographical distribution of the differences between NN and 1DVAR WTC ($2^{\circ} \times 2^{\circ}$ gridding average over the whole validation period).

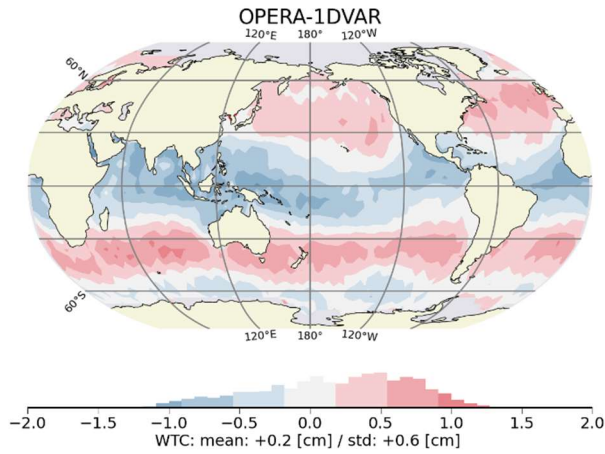


Figure 3-19 – Sentinel-3A: geographical distribution of the differences between NN and 1DVAR WTC (4°x4° gridding average over 4 years) [Source: AMTROC study funded by EUMETSAT].

Figure 3-20 shows the monitoring of the difference of SSH variance between the NN and 1DVAR approaches (left) and geographical distribution of the difference(right): negative values indicate that 1DVAR performs better. At global average, the NN approach performs slightly but constantly better than the 1DVAR by about 0.4 cm². This global analysis hides a more contrasted geographical distribution. The NN WTC performs better than 1DVAR WTC at latitudes larger than 30° where it is wetter than the 1DVAR (-0.5 cm² of variance reduction). Over the tropics, the two solutions show similar performances over clear-sky regions, and the situation is more contrasted over wetter regions with some areas where 1DVAR performs better than NN.

For comparison, Figure 3-21 shows the same metric for Sentinel-3 missions, where 1DVAR performs slightly but constantly better than the NN by about 0.2 cm² and where 1DVAR more clearly performs better over the Indo-Pacific warm pool and at latitudes higher than 50° while NN shows better performance in the mid-latitudes.

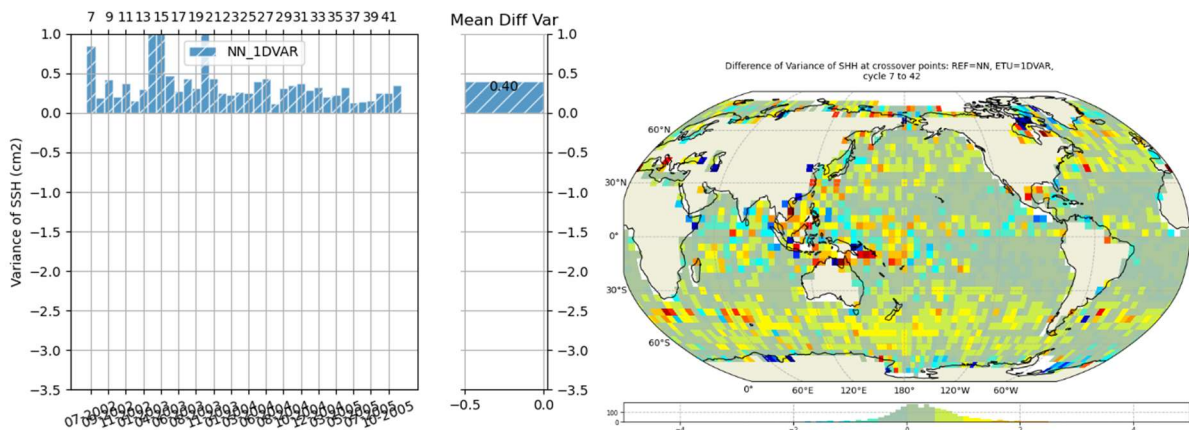


Figure 3-20 –ENVISAT: Monitoring of difference of SSH variance between N and 1DVAR approach (left) and geographical distribution of the difference(right). Negative values: 1DVAR performs better than NN, positive values: OPERA performs better than 1DVAR.

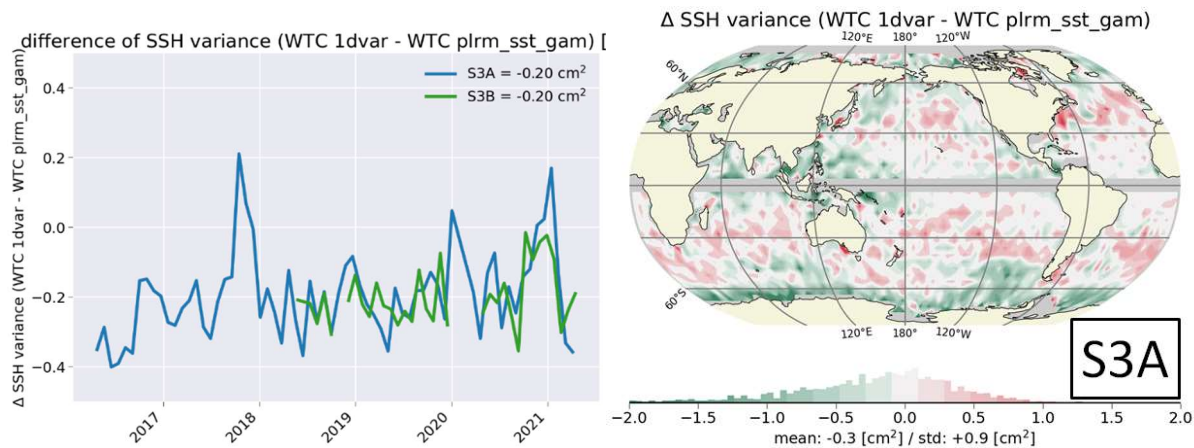


Figure 3-21 –Sentinel-3: monitoring of difference of SSH variance between 1DVAR and NN approach (left) and geographical distribution of the difference(right). Negative values: 1DVAR performs better than NN, positive values: OPERA performs better than 1DVAR.

3.4.3.3 Total column water vapour

Figure 3-22 shows TCWV averages from OPERA, 1DVAR, and ERA-5 for latitudinal zones of five degrees extension for one period in northern winter (left panel) and one in northern summer (right panel). Consistent differences between the three products can be observed: while there is a good agreement within the TCWV range of ca. 10-30 kg/m², 1DVAR shows increasingly higher TCWV values than ERA-5 above ca. 30 kg/m², while OPERA presents the exact opposite tendency. In the tropics, where the highest zonally averaged TCWV values are encountered, the TCWV difference 1DVAR – OPERA amounts to ca. 5 kg/m² with the ERA-5 values in between these two. This picture somewhat reverses for small TCWV concentrations, where 1DVAR shows lower values than OPERA.

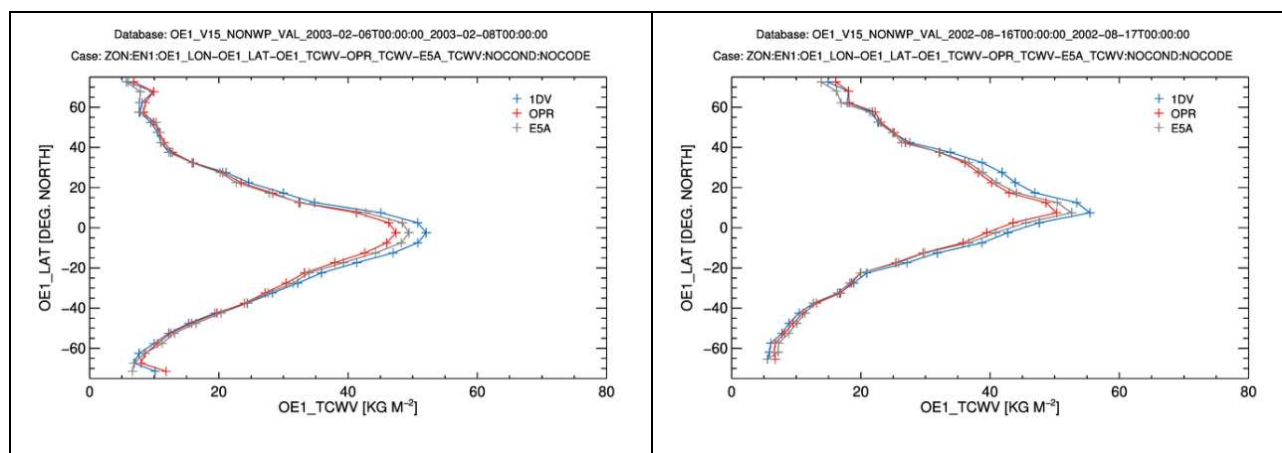


Figure 3-22 – ENVISAT: Zonal averages of 1DVAR (blue), OPERA (red), and ERA-5 (grey) TCWV retrievals in the northern winter (left, 6.-7. Feb. 2003, cycle 013, orbits 0662-0712) and northern summer (right, 16. Aug. 2002, cycle 008, orbits 0691-0719).

These principal differences are confirmed by the scattering plots shown in Figure 3-23 for another time period (23 July 2002). Again, OPERA is on average slightly drier than ERA-5 (TCWV bias of -0.65 kg/m²) while 1DVAR is wetter by about the same absolute amount (TCWV bias of +0.64 kg/m²), resulting in differing offsets and slopes if compared against ERA-5 with a smaller offset and a slope closer to 1 for OPERA. The correlation coefficients are almost identical with $r=0.980$ for OPERA vs. ERA-5 and $r=0.981$ for 1DVAR vs. ERA-5.

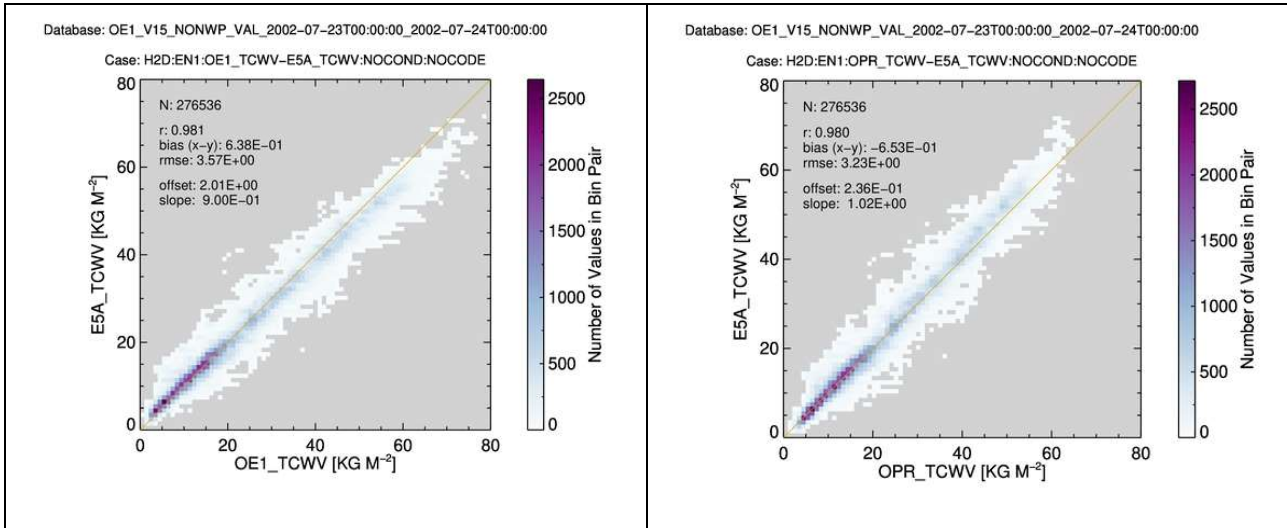


Figure 3-23 – ENVISAT: Two-dimensional histograms comparing the TCWV retrieval occurrences between 1DVAR and ERA-5 (left) as well as OPERA and ERA-5 (right) for 23 July 2002 (cycle 008, orbits 0003-0032).

Interestingly, there seems to be an upper boundary for OPERA TCWV retrievals at around 65 kg/m² (see Figure , right) which is not observed for 1DVAR and ERA-5. In order to investigate this issue closer, we have identified the orbit producing the highest TCWV values on 23 July 2002 (cycle 008, orbit 0004). Figure 3-24 shows the location of this specific (half-)orbit reaching from Kamchatka in the North to the Antarctic coast south of Australia. The highest TCWV values, exceeding 80 kg/m² for 1DVAR, reaching 75 kg/m² for ERA-5, and amounting to ca. 66 kg/m² for OPERA are found South-East of Japan. Analysing the corresponding meteorological situation, it turns out that the highest TCWV retrievals are associated with the presence of Cat-5 typhoon Feng-Shen, the most powerful typhoon of the 2002 Pacific storm season with central pressure values on the order of 920 mbar ([https://en.wikipedia.org/wiki/Typhoon_Fengshen_\(2002\)](https://en.wikipedia.org/wiki/Typhoon_Fengshen_(2002))). The 1DVAR retrieved TCWV values on the order of 80 kg/m² are therefore deemed plausible.

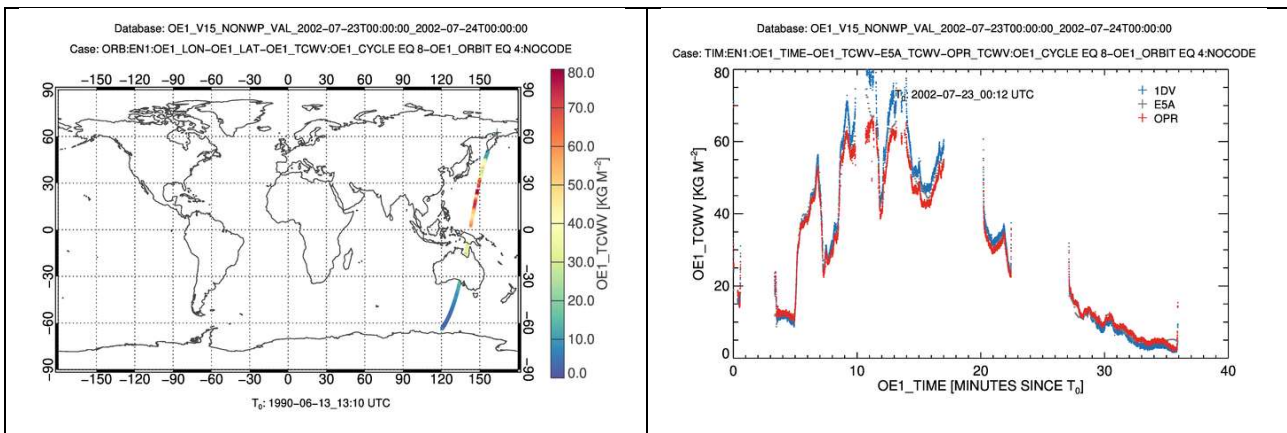


Figure 3-24 – ENVISAT. Left: 1DVAR TCWV along ENVISAT cycle 008, orbit 0004 (23 July 2002) projected on a map. Right: Comparison of 1DVAR (blue), OPERA (red), and ERA-5 (grey) TCWV values along the orbit shown in the left panel.

At high latitudes beyond 60° N/S, 1DVAR and OPERA TCWV retrievals are partly showing implausible TCWV increases (see e.g., Figure 3-22 left panel for zone 70° S), most likely due to retrievals affected by unidentified (and thus unmasked) sea ice. Similarly implausible TCWV retrievals are found near land-sea boundaries (see e.g., Figure 3-24, right panel, when the orbit reaches the Australian northern coast at around T₀+27 minutes or the Antarctic coast at T₀+36 minutes). This indicates that the 1DVAR quality flag has not been able to identify all problematic retrievals.

3.4.3.4 Atmospheric attenuation at Ku-band

The atmospheric attenuation at Ku-band (ATT_KU) is validated over the period covered by cycle 8 to cycle 13. Retrievals located at latitudes higher than 50° are edited in order to mitigate the impact of ice contamination.

The daily global average monitoring of the ATT_KU (see Figure 3-25, left) enables the comparison between NN (orange) and 1DVAR (blue) approaches. A bias of about 0.037 dB is observed between the two retrievals (Figure 3-25, right), with higher values for the NN. Following the drop of about -0.005 dB on the NN solution, a small increasing trend is observed on the difference, without further explanations for the moment.

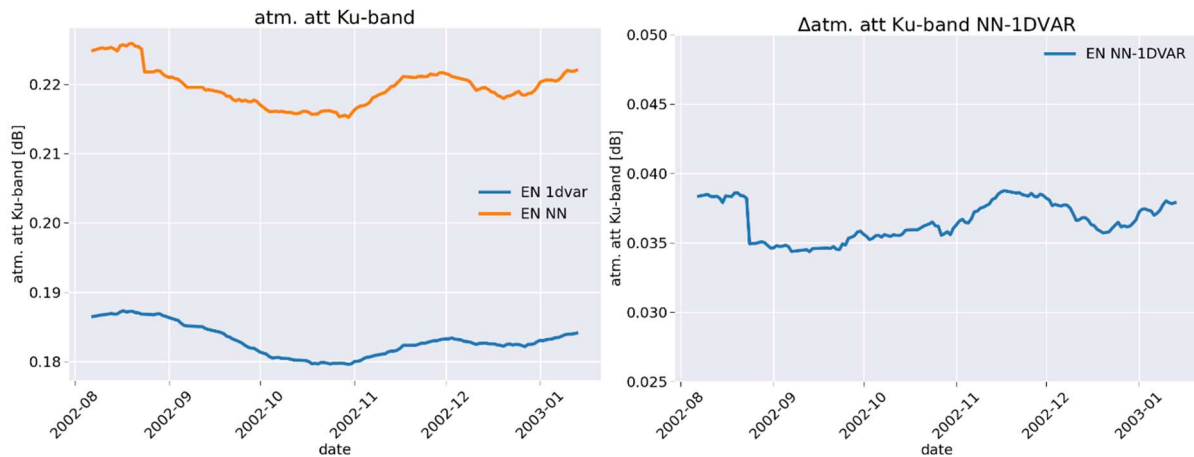


Figure 3-25 – ENVISAT: Daily global average monitoring of the atmospheric attenuation at Ku-band retrieved from the NN (orange) or the 1DVAR (blue) approach (left) and the differences between the two approaches (right). A 30-days moving average is applied to smooth the daily differences.

Figure 3-26 shows the geographical distribution of the differences between NN and 1DVAR ATT_KU (2°x2° gridding average over the whole validation period). Under predominantly clear sky conditions, the difference is small, below 0.02 dB. Under cloudy or precipitation conditions, the difference is larger and can reach values larger than 0.08 dB.

It is not possible for the moment to conclude which retrieval offers the better performance. In this respect, it would be interesting to compare the statistics of the retrievals against the expected values computed from a line-by-line or an empirical model to verify if one of the two solutions is closer to the theory.

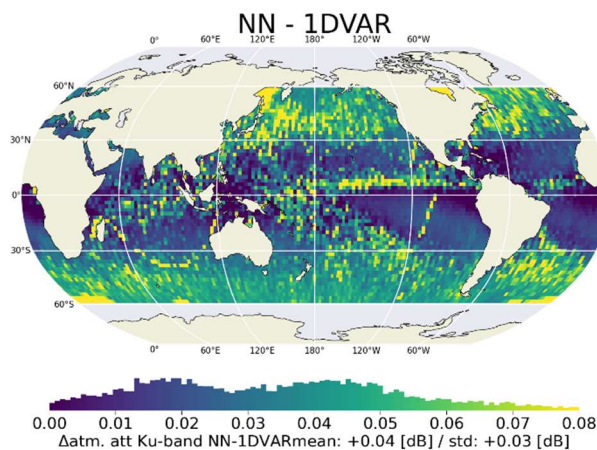


Figure 3-26 – ENVISAT: Geographical distribution of the differences between NN and 1DVAR ATT_KU (2°x2° gridding average over the whole validation period).

3.4.3.5 Liquid water path

Figure 3-27 (left) shows LWP averages from OPERA and 1DVAR for latitudinal zones of five degrees extension for the same two-day period (6.-7. Feb. 2003) in northern winter as shown for TCWV in Figure 3-22 (left). The overall picture is similar to what has already been observed for ERS-1/2: both products show a highly correlated zonal LWP distribution with a gap in absolute LWP retrieval of ca. 0.04 – 0.08 kg/m² (a bit smaller than for ERS-1/2) which appears to be widening with increasing LWP. The main reason for this gap lies in the fact that 1DVAR LWP retrievals are negatively biased (Figure 3-28, right), leading to negative LWP values in cloud-free areas, while OPERA LWP retrievals are positively biased (Figure 3-28, left) and negative OPERA LWP retrievals are set to 0.0 kg/m² leading to an additional positive bias in cloud-free areas. This can for example be observed in the Gulf of Carpentaria between Australia and New Guinea on 23 July 2002 (Figure 3-29, right panel, LWP at T0 plus 20-22 minutes), cloud-free at the time of the overpass as inferred from concomitant OLCI observations.

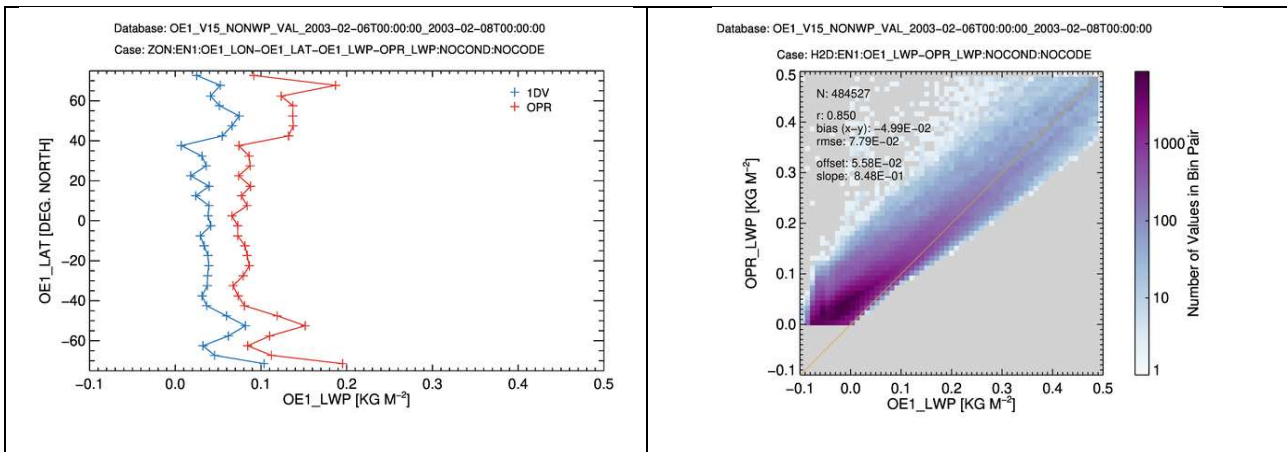


Figure 3-27 – ENVISAT. Left: Zonal averages of 1DVAR (blue) and OPERA (red) LWP retrievals in the northern winter (left, 6.-7. Feb. 2003, cycle O13, orbits 0662-0712. Right: Two-dimensional histograms comparing the LWP retrieval occurrences between 1DVAR and OPERA for the same period.

LWP locally shows much larger scatter than the rather smooth TCWV fields which is partly expected due to the often-irregular distribution of clouds and the relatively small effects of LWP on top-of-atmosphere brightness temperatures, enhancing the impact of noise on the retrieval.

The enforced lower boundary at LWP = 0.0 kg/m² for OPERA retrievals is clearly visible in Figure 3-27 (right) which also confirms the quite good correlation ($r=0.850$, but significantly lower than for ERS-1/2 with $r=0.920/0.942$) and the bias of 1DVAR-OPERA = -0.050 kg/m² (as compared to -0.087/-0.085 kg/m² for ERS-1/2) between the two retrievals.

This is further illustrated in Figure 3-28: since the cloud-free case is by far the most likely, the histograms should peak at LWP = 0.0 kg/m² with a retrieval-dependent scatter around this value. However, Figure 3-28 (left) shows that OPERA has a bias of at least +0.015 kg/m² (secondary (“true”) mode at +0.015 kg/m² plus additional increasing effect of forcing negative retrievals to zero). In contrast, 1DVAR has a negative bias of -0.015 kg/m² (Figure 3-28, right), resulting in the observed combined average difference LWP OPERA – LWP 1DVAR of ca. 0.040 - 0.080 kg/m².

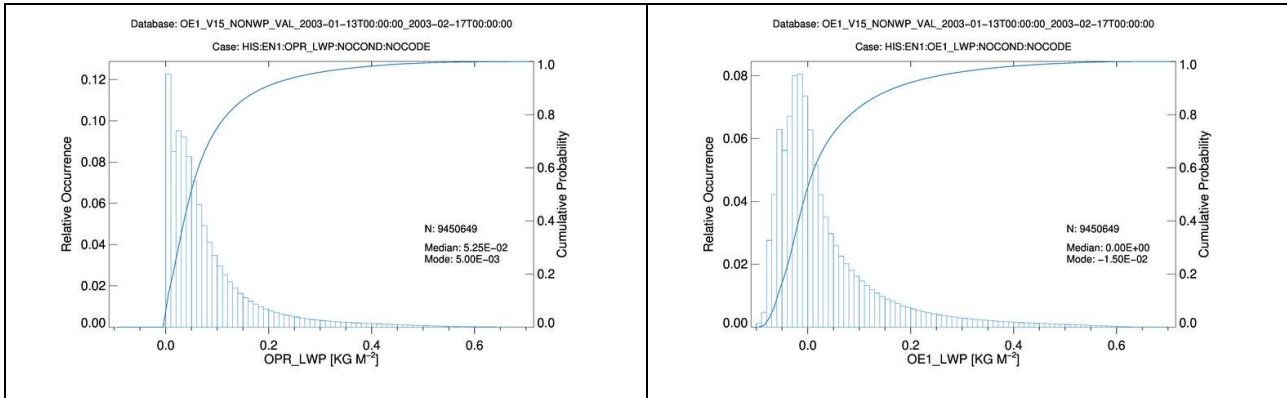


Figure 3-28 – ENVISAT. Left: Histogram of OPERA LWP for cycle 13 (13.1.- 17.2. 2003). Right: Same for 1DVAR LWP.

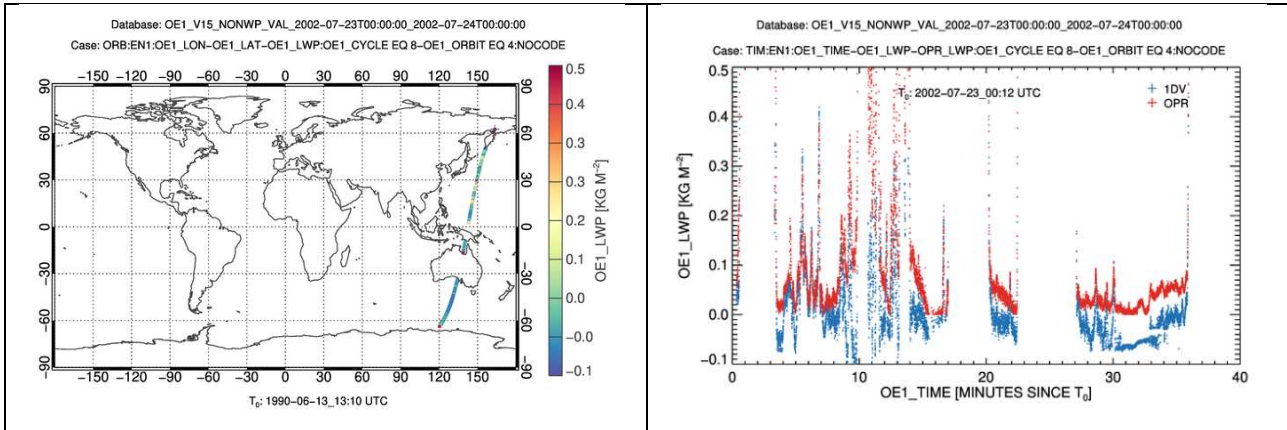


Figure 3-29 – ENVISAT. Left: 1DVAR LWP along ENVISAT cycle 008, orbit 0004 (23. July 2002) projected on a map. Right: Comparison of OPERA (red) and 1DVAR (blue) LWP values along the orbit shown in the left panel.

3.4.4 Summary

The validation of the Atmospheric TDP has shown generally consistent retrieval performance between the OPERA and 1DVAR retrieval on the one side and between ERS-1/2 and ENVISAT on the other side, with a few characteristic differences especially for LWP. Table 1 provides an overview of some key retrieval assessment parameters. A more detailed summary of the validation outcome is given in the parameter-specific subsections below.

Table 1 – Selected retrieval assessment parameters for the Atmospheric TDP as obtained from the specific validation cases presented herein.

	ERS-1	ERS-2	ENVISAT
WTC: Δ (OPERA – 1DVAR)	-2.5 mm	-2.5 mm	-4.0 mm
TCWV: r (OPERA, ERA-5)	0.979	0.983	0.981
TCWV: r (1DVAR, ERA-5)	0.983	0.986	0.980
TCWV: bias (OPERA – ERA-5)	-1.11 kg/m ²	-1.07 kg/m ²	+0.64 kg/m ²
TCWV: bias (1DVAR – ERA-5)	-0.74 kg/m ²	-0.61 kg/m ²	-0.65 kg/m ²
ATT_KU: Δ (OPERA – 1DVAR)	+0.035 dB	+0.035 dB	+0.037 dB
LWP: OPERA, mode	+0.025 kg/m ²	+0.025 kg/m ²	+0.025 kg/m ²
LWP: 1DVAR, mode	-0.055 kg/m ²	-0.055 kg/m ²	-0.015 kg/m ²

LWP: r (OPERA, 1DVAR)	0.942	0.920	0.850
-----------------------	-------	-------	-------

3.4.4.1 Miscellaneous

- ✓ 1DVAR quality flag:
 - The 1DVAR quality flag has proven useful to identify retrievals of good quality for subsequent evaluation.
 - Potential improvements of the 1DVAR quality flag concern better filtering of retrievals affected by contamination from land surfaces or sea ice.
- ✓ Discontinuity in OPERA ENVISAT products in August 2002:
 - A drop of about 1 mm is observed on the daily monitoring of the OPERA WTC around the end of August 2002.
 - A similar drop is observed for the other OPERA geophysical parameters.
 - The reasons behind this drop in the ENVISAT time series should be further investigated.
- ✓ While there is very good agreement between the investigated performance metrics for ERS-1 vs. ERS-2 retrievals, the corresponding metrics for ENVISAT do often somewhat differ from the former (see Table 1 above), hinting at some differences either in the MWR raw data or in the Level-1B processing for ENVISAT.

3.4.4.2 Wet tropospheric correction:

- ✓ OPERA and 1DVAR shows similar results with a global WTC bias of about 4 mm between the two retrievals at global scales, but with stronger zonally distributed differences:
 - 1DVAR WTC is wetter than the OPERA WTC over the tropics,
 - OPERA WTC is wetter than the 1DVAR WTC at higher latitudes.
- ✓ Looking at the SSH variance at crossovers, OPERA performs slightly better than 1DVAR by about 0.4 cm².
 - Similar results are observed for the Sentinel-3 missions, where however 1DVAR performs slightly better than OPERA by about 0.2 cm².
 - The regions where OPERA or 1DVAR performs better could be related to the observed WTC bias.
- ✓ Further studies are required to better understand the observed differences in WTC, which, in turn, could lead to improved performances for both approaches.

3.4.4.3 Total column water vapour

- ✓ OPERA and 1DVAR are in excellent agreement both with each other and with ERA-5 in the TCWV range from 10 to 30 kg/m².
- ✓ In general, it is difficult to tell whether OPERA or 1DVAR is more accurate due to the limited availability of high-quality independent reference data (radiosonde or GNSS-based) over the open ocean for the period of interest (1993-2002).
- ✓ 1DVAR shows systematically higher TCWV values as compared to ERA-5 TCWV in very moist atmospheres, while OPERA TCWV values are lower under such conditions.
 - Analysing ENVISAT observations of a large tropical storm, 1DVAR TCWV appears to provide the more accurate retrievals for extremely moist atmospheres.
- ✓ Land or sea ice contamination leads to significant TCWV overestimation for both OPERA and 1DVAR retrievals, underpinning the high importance of reliable product quality flag (see above).
- ✓ High quality GPS-based independent TCWV reference data comprising a significant number of near-coast sites are meanwhile available for the Sentinel-3 era [RD 54]. Further insight in retrieval

performance can therefore be obtained by applying both retrieval methods to observations of the almost identical MWR instruments onboard the Sentinel-3 series of satellites. Such investigations are currently carried out in the frame of EUMETSAT’s AMTROC project [RD 2].

3.4.4.4 Atmospheric attenuation in the Ku band

- ✓ A bias of 0.04 dB is observed on the difference between OPERA and 1DVAR retrieval (OPERA larger).
- ✓ Further insight into ATT_KU retrieval quality could be obtained by comparing the retrieval statistics against theoretical models (line-by-line or empirical).

3.4.4.5 Liquid water path

- ✓ LWP retrieval is noisy for both OPERA and 1DVAR, mainly due to irregular cloud cover and the limited information content of the 23 and 36 GHz brightness temperatures as regards LWP.
- ✓ OPERA and 1DVAR resolve dynamic LWP structures similarly but differ in their absolute values by an average difference of -0.05 kg/m² to -0.10 kg/m² of 1DVAR LWP (drier) as compared to OPERA LWP (wetter).
- ✓ Consequently, FDR4ALT LWP products are deemed suitable in its current state only to provide information on e.g., LWP gradients or trends, but should not be used to provide absolute values.
- ✓ There appear to be two reasons for the observed differences:
 - The retrievals themselves are characterised by a dry bias of ca. -0.02 kg/m² for 1DVAR, respectively a wet bias of ca. +0.02 kg/m² for OPERA.
 - Further wet bias of ca. +0.01 kg/m² is added to the OPERA retrieval due to setting the lower retrieval boundary to zero, i.e., to not allow for negative LWP retrievals.
- ✓ As a first step towards improving LWP retrieval quality, the respective reasons for the observed LWP biases should be investigated in more detail.

3.4.5 Reference documents

RD 1	Yuan, P., Blewitt, G., Kreemer, C., Hammond, W. C., Argus, D., Yin, X., Van Malderen, R., Mayer, M., Jiang, W., Awange, J., and Kutterer, H.: An enhanced integrated water vapour dataset from more than 10 000 global ground-based GPS stations in 2020, <i>Earth Syst. Sci. Data</i> , 15, 723–743, https://doi.org/10.5194/essd-15-723-2023 , 2023.
RD 2	https://www.eumetsat.int/AMTROC , last accessed 2023-04-15.

3.5 Difference of variance of SSH at crossover points

Difference of variance of Sea Surface Height at crossover points is a common tool to assess the performances of a correction with respect to another correction or a reference common with other instruments. In this diagnosis, corrections and filtering of data is very important. In terms of filtering, we use the validity flag provided by the Ocean & Coastal TDP, as well as threshold criteria on both WTC, and distance to shoreline criteria. The wet tropospheric correction was averaged from 7Hz to 1Hz using the same algorithm for both corrections, and quality flags were used to select the data to be averaged.

Sea Surface Height computed with ANN is compared to SSH computed with 1DVAR retrieved WTC. Crossover points with a time difference lower than 10 days are selected, and the difference of variance is computed. One solution is chosen to be the reference and the other solution will be compared to the reference. The difference of variances is thus computed as $\text{Var}(\text{SSH}(\text{WTC}_{\text{etu}})) - \text{Var}(\text{SSH}(\text{WTC}_{\text{ref}}))$. If the new correction improves the performances according to this criterion, the difference will be negative, as the variance of SSH

will be reduced with respect to the reference. On the contrary, if the new solution does not improve, the difference will be positive.

In the analyses presented hereafter, ANN WTC is selected as the reference. Consequently, we will analyze the difference $\text{Var}(\text{SSH}(\text{WTC_1DVAR})) - \text{Var}(\text{SSH}(\text{WTC_ANN}))$

Two diagnostics will be presented: timeseries of difference of variance for all crossover points (global), and for low oceanic variability areas (SL2). In these timeseries, one point of the curves stands for the difference of variance for one cycle.

Maps of difference provide an illustration of the geographical improvement in performances. Indeed, one solution may show better performances one some areas, but lower performances for other. Crossover points are gridded in $2^\circ \times 2^\circ$ boxes and the variance is computed for all boxes. The colormap on these maps is such that yellow/red indicates a degradation of performances (positive difference) and light blue/blue indicates an improvement of performances (negative difference).

3.5.1 ENVISAT

Figure 3-30 illustrates the impact on the performances when using ANN solution versus FMRV3 correction for the ENVISAT mission from cycle 7 to cycle 112. **ANN correction improves the performances with respect to the FMR correction over ocean of -0.88cm^2** in average over the whole timeseries. The improvement is not constant along the 10 years of data but presents a slope with an improvement around -1.0cm^2 in the first years, and around -0.5cm^2 in the last years. Selection over low oceanic variability presents an improvement slightly lower of -0.72cm^2 meaning that the ANN has more impact on the high variability areas. The map of the difference shows that the improvement is brought mainly by the high latitudes, while the performance is quite similar in the tropical area.

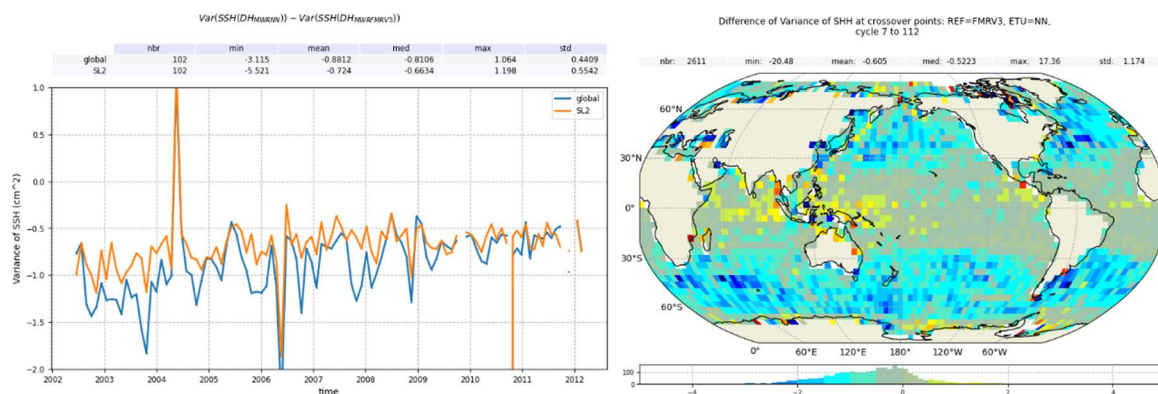


Figure 3-30: ENVISAT : FMR V3 vs ANN analysis by Difference of variance of SSH at crossover points

Figure 3-31 illustrates the impact on the performances when using 1DVAR solution versus FMRV3 correction. 1DVAR correction improves the performances over ocean of -0.65cm^2 in average over the whole timeseries. The timeseries presents a slope similar to the one observed with the ANN solution. Selection over low oceanic variability presents an improvement slightly lower of -0.5cm^2 . The map of the difference shows similar pattern that the ANN correction with a lower amplitude in the high latitudes.

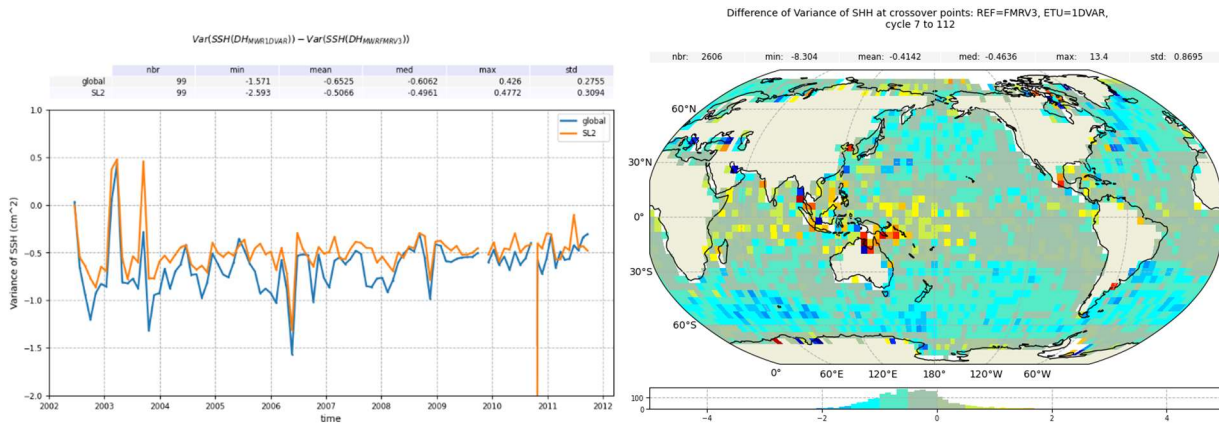


Figure 3-31: ENVISAT : FMR V3 vs 1DVAR analysis by Difference of variance of SSH at crossover points

Figure 3-32 illustrates the impact on the performances when using ANN solution versus 1DVAR solution for the ENVISAT mission from cycle 7 to cycle 107. The timeseries show a difference of variance positive over the whole period. But some variations can be observed. Some cycles at the beginning of the period show some spurious values, while the average difference seems to be slightly higher than 0.25cm². The cycles with the spurious values should be analyzed further to discard any acquisition or editing issue. In the middle of the timeseries, the average difference seems lower than 0.25cm².

The map of difference of variances shows that the ANN performs better in the areas between 30°-60° for both hemispheres. 1DVAR performs better in the dry areas (near Antarctica) and in very wet and cloudy atmospheres (south east asia).

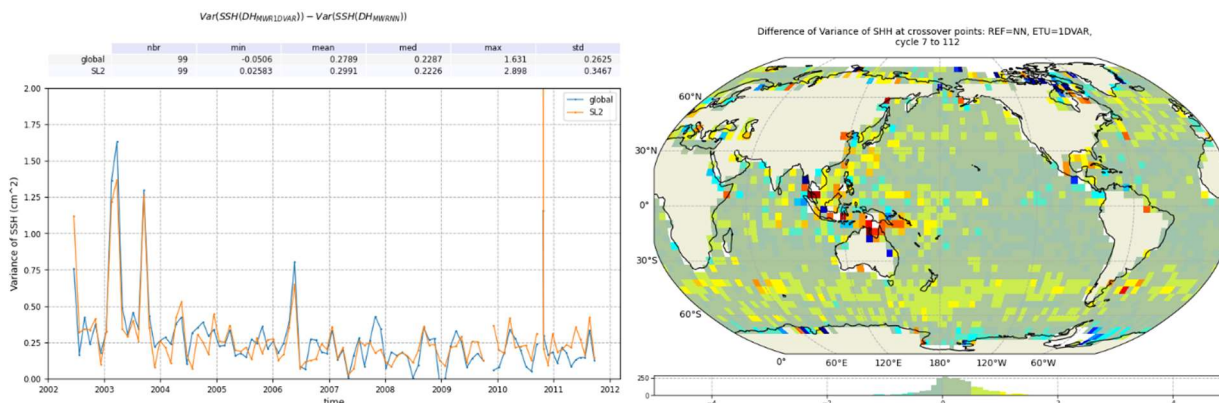


Figure 3-32: ENVISAT: 1DVAR vs ANN analysis by Difference of variance of SSH at crossover points

3.5.2 ERS-2

Figure 3-33 illustrates the impact on the performances when using ANN solution versus the REAPER V2 correction solution for the ERS-2 mission from cycle 1 to cycle 85. **ANN correction improves the performances with respect to the REAPER correction over ocean of -1.19cm² in average over the whole timeseries.** The improvement is quite constant along the 10 years of data. Selection over low oceanic

variability presents an improvement slightly higher of -1.5cm^2 . The map of the difference shows that the improvement is global over ocean, with patches of higher improvements in the tropical area. There is a band of small degradation of performances in a band between -60° and -40° in the south hemisphere.

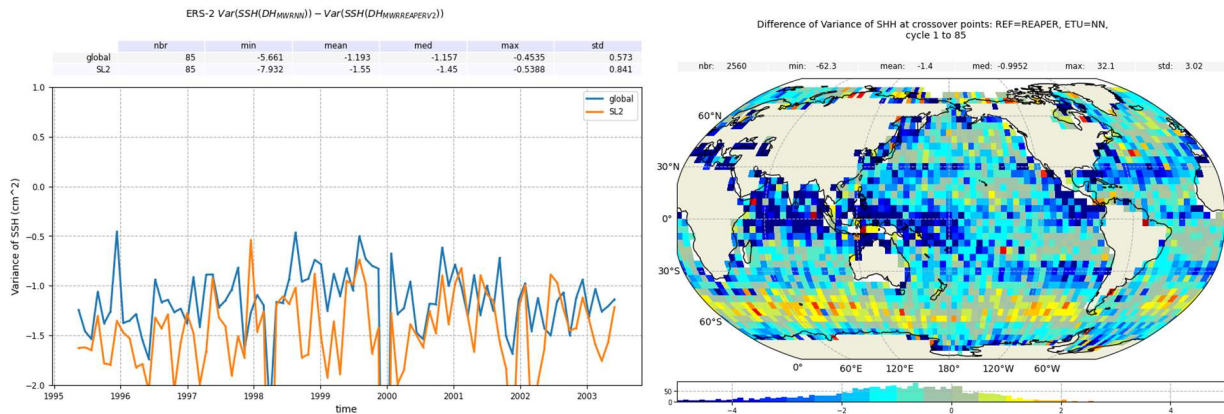


Figure 3-33: ERS-2: REAPER vs ANN analysis Difference of variance of SSH at crossover points

Figure 3-34 illustrates the impact on the performances when using 1DVAR solution versus REAPER V2 solution. **1DVAR correction improves the performances with respect to the REAPER correction over ocean of -0.58cm^2** in average over the whole timeseries. The improvement is not constant along the 10 years of data but presents a slope with an improvement around -1.0cm^2 in the first years, and around -0.2cm^2 in the last years. Selection over low oceanic variability presents an improvement slightly higher of -0.83cm^2 . The map of the difference shows that the improvement is global over ocean, with patches of higher improvements in the tropical area. There is a band of small degradation of performances in a band between -60° and -40° in the south hemisphere. Geographical patches are really similar to the ones observed with the ANN correction. The 60S-40S band would need further analyses to understand the root cause of this degradation.

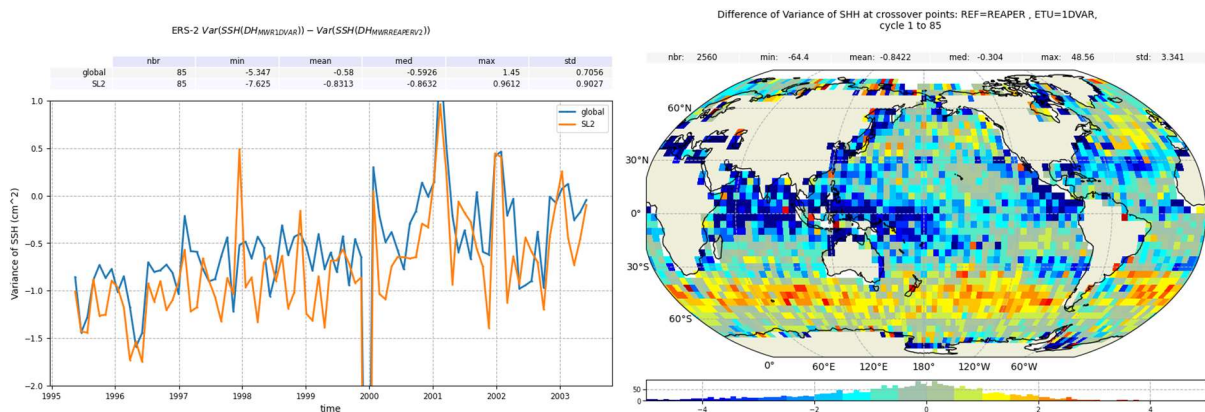


Figure 3-34: ERS-2: REAPER vs 1DVAR analysis by Difference of variance of SSH at crossover points

Figure 3-35 illustrates the impact on the performances when using ANN solution versus 1DVAR solution. The results are consistent with the previous observations on the difference between both FDR4LAT corrections and the REAPER V2 correction.

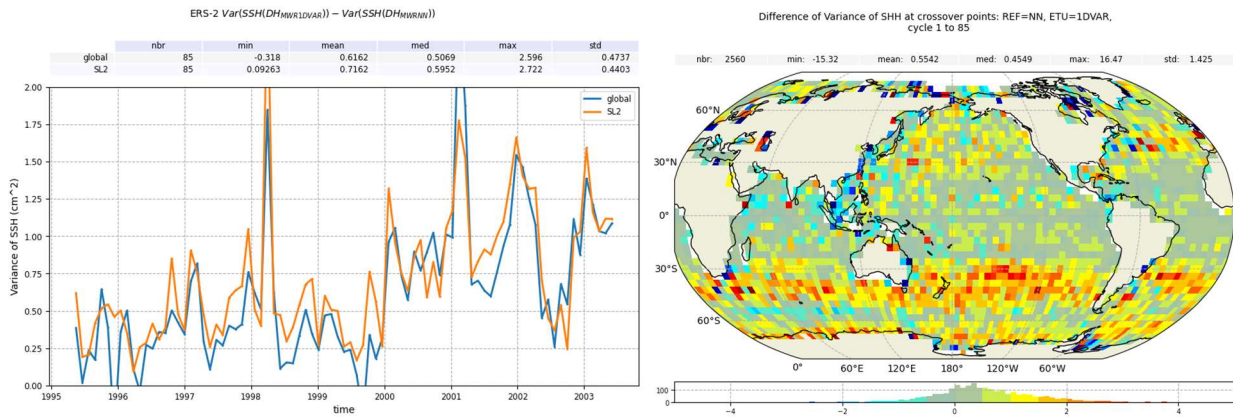


Figure 3-35: ERS-2: 1DVAR vs ANN Difference of variance of SSH at crossover points

3.5.3 ERS-1

The beginning of the timeseries was not analyzed because the selected Dynamic Atmospheric Correction (DAC) solution is not available prior to February 1992. We chose also to analyze only cycles of 35 days or more. Indeed, ERS-1 mission is very peculiar on that point, with cycles from 3 days to 167 days. Consequently, ERS-1 data was analyzed from cycle 64 to cycle 156.

Figure 3-36 illustrates the impact on the performances when using ANN solution versus REAPER V2 solution. **ANN correction improves the performances with respect to the REAPER correction over ocean of -0.91cm²** in average over the whole timeseries. Over low oceanic areas, the improvement is -1.27cm² in average. The map of the difference shows that the main improvements are observed in the tropical area, while a small band of degradation is observed in the south hemisphere as observed in ERS-2 results.

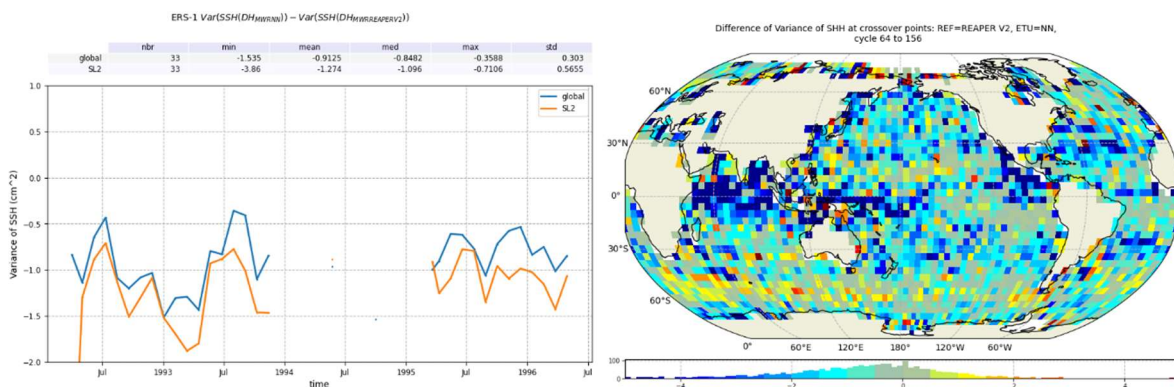


Figure 3-36: ERS-1 : REAPER vs ANN Difference of variance of SSH at crossover points

Figure 3-37 illustrates the impact on the performances when using 1DVAR solution versus REAPER V2 solution. **1DVAR correction improves the performances with respect to the REAPER correction over ocean of -0.54cm²** in average over the whole timeseries. Over low oceanic areas, the improvement is -0.94cm² in average. The map of the difference show that the main improvement is observed in the tropical area, while a small band of degradation is observed in the south hemisphere as observed in ERS-2 results.

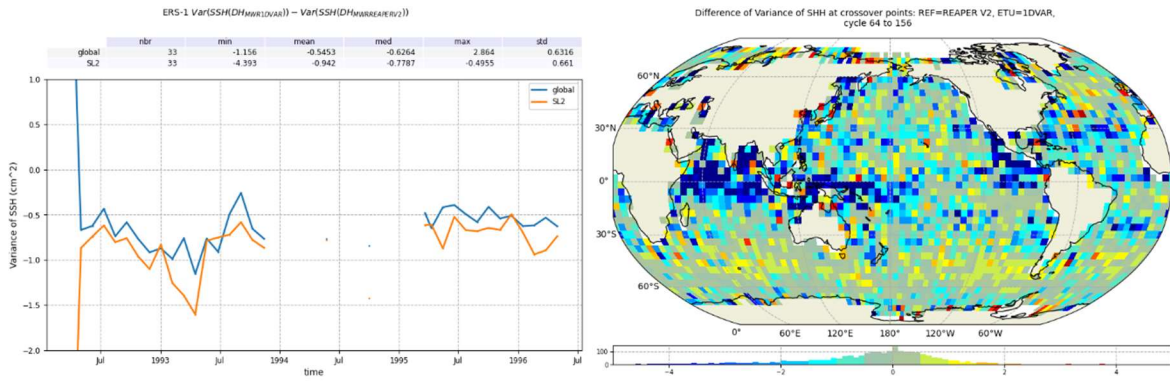


Figure 3-37: ERS-1: REAPER vs 1DVAR Difference of variance of SSH at crossover points

Figure 3-38 illustrates the impact on the performances when using ANN solution versus 1DVAR solution for the ERS-1 mission. The results are consistent with the previous observations on the difference between both FDR4LAT corrections and the REAPER V2 correction.

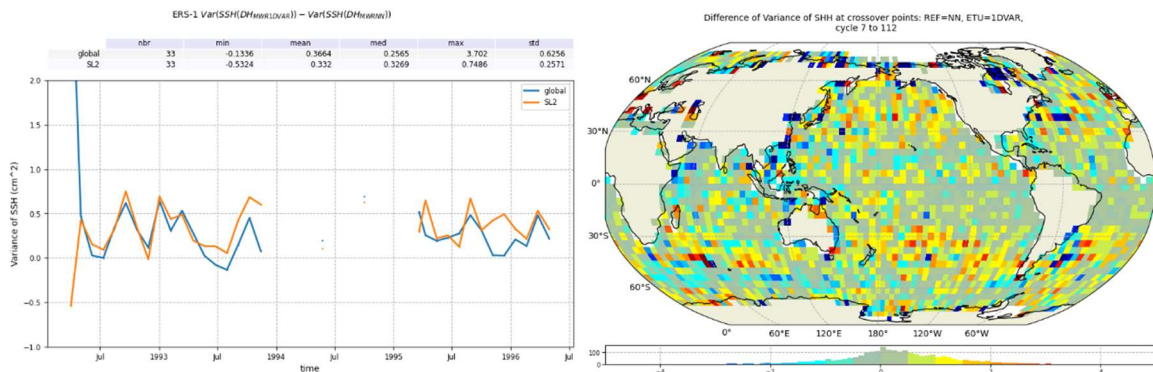


Figure 3-38: ERS-1: 1DVAR vs ANN Difference of variance of SSH at crossover points

3.6 Conclusion and Remarks

Difference of variance of Sea Surface Height is a common tool to assess the performances of a correction with respect to another correction or a reference common with other instruments. Sea Surface Height computed with ANN or 1DVAR has been compared to SSH computed with previous reprocessing correction.

- ENVISAT
 - ANN vs FMRV3: -0.88cm^2
 - 1DVAR vs FMRV3: -0.65cm^2
- ERS-2
 - ANN vs REAPER : -1.5cm^2
 - 1DVAR vs REAPER: -0.58cm^2
- ERS-1
 - ANN vs REAPER : -0.91cm^2
 - 1DVAR vs REAPER: -0.54cm^2

Both wet tropospheric corrections proposed in the FDR4ALT Atmospheric TDP improve the performances with respect to previous reprocessing, according to this diagnostic. Better performances are achieved by ANN correction for three missions.

Appendix A - FDR4ALT deliverables

The table below lists all FDR4ALT deliverables with their respective ID number and confidentiality level.

Document	ID	Confidentiality Level
Products Requirements & Format Specifications Document	[D-1-01] [D-2-02]	Public
Roadmap & Product Summary Document	[D-1-02]	Project Internal
Data Requirements Document	[D-1-03]	Project Internal
System Maturity Matrix	[D-1-04]	Project Internal
Examples of products	[D-1-05]	Project Internal
Review Procedure Document	[D-1-06]	Project Internal
Review Data Package	[D-1-07]	Project Internal
Phase 1 Review Report Document	[D-1-08]	Project Internal
Detailed Processing Model Document	[D-2-01]	Public
Round Robin Assessment Report Document	[D-2-03]	Public
Data Production Status Report	[D-3-01]	Project Internal
Final Output Dataset	[D-3-01]	Public
Product Validation Plan	[D-4-01]	Project Internal
Product Validation Report : FDR	[D-4-02a]	Public
Product Validation Report : Sea-Ice TDP	[D-4-02b]	Public
Product Validation Report: Land-Ice TDP	[D-4-02c]	Public
Product Validation Report : Ocean Waves TDP	[D-4-02d]	Public
Product Validation Report : Ocean & Coastal TDP	[D-4-02e]	Public
Product Validation Report: Inland Waters TDP	[D-4-02f]	Public
Product Validation Report: Atmosphere TDP	[D-4-02g]	Public
Uncertainty Characterization Definition Document	[D-5-01]	Project Internal
Uncertainty Characterization Report	[D-5-02]	Public
Product User Guide	[D-5-03]	Public
Completeness Report ALT	[D-7-01]	Public
Completeness Report MWR	[D-7-02]	Public

Table 2 : List of FDR4ALT deliverables

Appendix B - Acronyms

AATSR	Advanced Along-Track Scanning Radiometer
AEM	Airborne electromagnetic
AIR	AIRWAVES2
AVISO	Archivage, Validation et Interprétation des données des Satellites Océanographiques
AMSR-E	Advanced Microwave Scanning Radiometer - Earth Observing System sensor
AMSU-A	Advanced Microwave Sounding Unit-A
ALT	Altimetry
ASSIST	Arctic Shipborne Sea Ice Standardization Tool
ATM	Airborne Topographic Mapper
BDHI	Base de datos Hidrologica integrada
BGEP	Beaufort Gyre Exploration Project
CAL	Calibration
CCI	Climate Change Initiative
CFOSAT	Chinese-French Oceanic SATellite
CDS	Copernicus Data Service
CLS	Collecte Localisation Satellite
CMEMS	Copernicus Marine Environment Monitoring Service
CMSAF	Climate Monitoring Satellite Application Facility
CNES	Centre National des Etudes Spatiales
CRREL	Cold Regions Research and Engineering Laboratory
DAHITI	Database for Hydrological Time Series of Inland Waters
DGA	Dirección General de Aguas
ENVISAT	ENVironment SATellite
EMD	Empirical mode decomposition
EO	Earth Observation
EPS	European Polar System
ERA	ECMWF Re-Analysis
ERS	European Remote-Sensing Satellite
ESA	European Space Agency
ESTEC	European Space Research and Technology Centre
FCDR	Fundamental Climate Data Record
FDR	Fundamental Data Records
FIDUCEO	Fidelity and uncertainty in climate data records from Earth Observations
FMR	Full Mission Reprocessing
FYI	First Year Ice
GEWEX	Global Energy and Water Exchanges
GFO	Geosat Follow-On
GIEMS	Global Inundation Extent from Multi-Satellites
GMSL	Global Mean Sea Level
GNSS	Global Navigation Satellite System
GPM	Global Precipitation Measurement
GRDC	Global Runoff Data Centre
G-REALM	Global Reservoir And Lake Monitor
G-VAP	GEWEX Water Vapour Assessment
HYBAM	HYdro-géochimie du Bassin AMazonien
ICARE	

IGM	Instituto Geografico Militar
IGN	Instituto Geografico Nacional
IMB	Ice Mass Balance
INA	Instituto Nacional de Agua
ISRO	Indian Space Research Organisation
IRPI	Istituto di Ricerca per la Protezione Idrogeologia
IWMI	International Water Management Institute
LEGOS	Laboratoire d'Etudes en Géophysique et Océanographie Spatiales
LIDAR	Ligth Detection And Ranging
LTAN	Local time of the ascending node
LWP	Liquid Water Path
MAC	Multisensor Advanced Climatology
MEAS-SIM	Measure-Simulation
MQE	Mean Quadratic Error
MSSH	Mean Sea Surface Height
MWR	Microwave Radiometer
NASA	National Aeronautics and Space Administration
NE	North East
NN	Neural Network
NPI	Norwegian Polar institute
NWP	Numerical Weather Prediction
NOAA	National Oceanic and Atmospheric Administration
OIB	Operation Ice Bridge
OLC	Open Loop Calibration
OSTST	Oceanography Surface Topography Science Team
POSTEL	Pôle d'Observation des Surfaces continentales par TELEdetection
PTR	Point Target Response
RD	Reference Document
REAPER	Reprocessing of Altimeter Products for ERS
RM	Review Meeting
RSS	Remote Sensing System
SALP	Service d'Altimétrie et de Localisation Précise
SARAL	Satellite with Argos and Altika
SLA	Sea Level Anomaly
SCICEX	Submarine Arctic Science Program
SGDR	Sensor Geophysical Data Record
SHOA	Servicio Hidrografico y Oceanografico de la Armada
SSB	Sea State Bias
SSH	Sea Surface Height
SSM/I	Special sensor microwave/imager
SST	Sea Surface Temperature
SWH	Significant Wave Height
SWIM	Surface Waves Investigation and Monitoring instrument
TAC	Thematic Assembly Center
TB	Température de Brillance (Brightness Temperature)
TDP	Thematic Data Products
TDS	Test Data Set
TFMRA	Threshold First-Maximum Retracker Algorithm
TMR	Topex Microwave Radiometer
TP	Topex/Poseidon

TCWV	Total column water vapour
VCC	Vicarious calibration
VS	Virtual Station
ULS	Upward Looking Sonar
USA	United States of America
USDA	United States Department of Agriculture
WHALES	Wave Height Adaptive Leading Edge Subwaveform
WTC	Wet Tropospheric Correction

